

FACULDADE DE BIOCÉNIAS
PROGRAMA DE PÓS-GRADUAÇÃO EM BIOLOGIA CELULAR E MOLECULAR
MESTRADO EM BIOLOGIA CELULAR E MOLECULAR

JOSÉ EDUARDO SACCONI NUNES

**A ENZIMA HISTIDINOL DESIDROGENASE DE *MYCOBACTERIUM TUBERCULOSIS* COMO ALVO
PARA O DESENVOLVIMENTO DE DROGAS: CARACTERIZAÇÃO BIOQUÍMICA**

Porto Alegre
2011

PÓS-GRADUAÇÃO - *STRICTO SENSU*



Pontifícia Universidade Católica
do Rio Grande do Sul

Ficha Catalográfica

N972e Nunes, José Eduardo Sacconi

A Enzima Histidinol Desidrogenase de Mycobacterium tuberculosis como Alvo para o Desenvolvimento de Drogas : Caracterização Bioquímica / José Eduardo Sacconi Nunes . – 2011.

41 p.

Dissertação (Mestrado) – Programa de Pós-Graduação em Biologia Celular e Molecular, PUCRS.

Orientador: Prof. Dr. Diógenes Santiago Santos.

Co-orientador: Prof. Dr. Luiz Augusto Basso.

1. Tuberculose. 2. Histidinol Desidrogenase. 3. Desenho Racional de Fármacos. 4. Cinética Enzimática. I. Santos, Diógenes Santiago. II. Basso, Luiz Augusto.
III. Título.

Elaborada pelo Sistema de Geração Automática de Ficha Catalográfica da PUCRS

com os dados fornecidos pelo(a) autor(a).

Bibliotecária responsável: Salete Maria Sartori CRB-10/1363



Pontifícia Universidade Católica do Rio Grande do Sul
Faculdade de Biociências
Programa de Pós-Graduação em Biologia Celular e Molecular

DISSERTAÇÃO DE MESTRADO

JOSÉ EDUARDO SACCONI NUNES

**A Enzima Histidinol Desidrogenase de *Mycobacterium tuberculosis* como
Alvo para o Desenvolvimento de Drogas: Caracterização Bioquímica**

Porto Alegre
2011

JOSÉ EDUARDO SACCONI NUNES

**A Enzima Histidinol Desidrogenase de *Mycobacterium tuberculosis* como
Alvo para o Desenvolvimento de Drogas**

Dissertação apresentada como
requisito para a obtenção do
grau de Mestre pelo programa
de Pós-Graduação em Biologia
Celular e Molecular da Pontifícia
Universidade Católica do Rio

Orientador:

Prof. Dr. Diógenes Santiago Santos

Co-orientador:

Prof. Dr. Luiz Augusto Basso

Porto Alegre

2011

AGRADECIMENTOS

Primeiramente gostaria de agradecer a Deus. Sem ele pra me guiar e dar força eu não teria chegado a lugar nenhum.

À minha família pelo apoio e estrutura, pelo amor dedicado e incentivo sempre para que me tornasse um profissional melhor.

Ao Prof. Dr. Diógenes Santiago Santos, pela oportunidade, aprendizado, incentivo e confiança depositados e também pelo exemplo de cientista perseverante e realizador.

Ao Prof. Dr. Luiz Augusto Basso, pelo conhecimento compartilhado e auxílio fundamental na discussão dos resultados.

À Dra. Jocelei Maria Chies, por todas as conversas, incentivo, compreensão com os horários e bons momentos compartilhados.

Aos colegas na empresa Quatro G Pesquisa & Desenvolvimento, por todo auxílio prestado, pela compreensão com os horários e fundamental alegria e amizade no ambiente de trabalho. Em especial à Gaby Renard e Cláudia Paiva Nunes, pelo apoio nos momentos difíceis.

Aos colegas do Centro de Pesquisas em Biologia Molecular e Funcional, pelo conhecimento compartilhado, pelo auxílio nos experimentos e pela amizade. Em especial aos colegas Rodrigo Ducati e Ardala Breda que tiveram contribuição fundamental nos resultados e formato desse trabalho.

Aos amigos Júnior, Luiza, Thiago e Fernando, pelos conselhos, momentos de descontração e apoio que com certeza tornaram realizar esse trabalho muito mais fácil e divertido.

LISTA DE ABREVIATURAS:

AICAR: 5'-fosphoribosil-4-carboxamide-5-aminoimidazol

AIDS: *acquired immune deficiency syndrome* ou síndrome da imunodeficiência adquirida.

BCG: *bacilli Calmette-Guérin* ou bacilo de Calmette e Guérin.

DNA: *Deoxyribonucleic acid* ou Ácido Desoxirribonucléico

DMSO: dimetilsulfóxido.

DOTS: *directly observed treatment short-course* ou terapia de curta duração diretamente observada.

HIV: *human immunodeficiency virus* ou vírus da imunodeficiência humana.

HPLC: *high performance liquid chromatography* ou cromatografia líquida de alta performance.

IAP: Imidazol-Acetyl-Fosfato

IGP: Imidazol-Glicerol-Fosfato

L-Hol: L-Histidinol

L-Hol-P: L-Histidinol-Fosfato

MDR-TB: *multidrug-resistant tuberculosis* ou tuberculose resistente a múltiplas drogas.

OMS: Organização Mundial da Saúde.

ORF: *open reading frame* ou fase de leitura aberta

PCR: *polymerase chain reaction* ou reação em cadeia da polimerase.

PPD: *purified protein derivate* ou derivado purificado de proteína.

TB: Tuberculose

XDR-TB: *Extensively Drug Resistant Tuberculosis* ou Tuberculose Extensivamente Resistente a Drogas.

SUMÁRIO:

CAPÍTULO 01

1.	INTRODUÇÃO	II
1.1	A TUBERCULOSE	II
1.2.	O MYCOBACTERIUM TUBERCULOSIS	V
1.3.	RESISTÊNCIA A MÚLTIPAS DROGAS	VII
1.4.	BIOSSÍNTESE DE HISTIDINA E <i>HISD</i>	VIII

CAPÍTULO 02

2.	OBJETIVOS	XIII
2.1.	OBJETIVO GERAL	XIII
2.2.	OBJETIVOS ESPECÍFICOS	XIII

CAPÍTULO 03

3.	ARTIGO SUBMETIDO AO ARCHIVES OF BIOCHEMISTRY AND BIOPHYSICS MOLECULAR, KINETIC, THERMODYNAMIC, AND STRUCTURAL ANALYSES OF MYCOBACTERIUM TUBERCULOSIS HISD-ENCODED METAL-DEPENDENT DIMERIC HISTIDINOL DEHYDROGENASE (EC 1.1.1.23)	143
----	---	-----

CAPÍTULO 04

4.	CONSIDERAÇÕES FINAIS	XVI
----	----------------------	-----

BIBLIOGRAFIA

XVIII

RESUMO

Em 2009 a tuberculose (TB) foi responsável por 1,3 milhões de mortes no mundo inteiro. A incidência de casos chegou ao patamar de 9,4 milhões e as estimativas da Organização Mundial da Saúde (OMS) indicam que aproximadamente 1/3 da população mundial está infectada pelo *Mycobacterium tuberculosis*, principal agente causador da doença. A falta de novas drogas no mercado, o tratamento longo e com efeitos colaterais (levando ao abandono por parte dos pacientes) e os quadros de co-infecção com HIV tem colaborado para o surgimento de novas cepas resistentes as drogas atualmente em uso (MDR-TB e XDR-TB). Fica claro, portanto, que o desenvolvimento de novas drogas para o combate da TB é necessário e fundamental para que se tenha sucesso na erradicação desta doença. A via de biossíntese de histidina aparece nesse contexto oferecendo alvos atrativos, visto que está presente em organismos procarióticos, em organismos eucarióticos inferiores e em plantas, mas ausente em animais. A última enzima pertencente à via é chamada de Histidinol Desidrogenase e é responsável pela conversão de L-Histidinol em L-Histidina. Sua essencialidade para a viabilidade do bacilo foi comprovada através de nocaute gênico, confirmando sua potencialidade para o desenvolvimento de compostos inibidores de sua atividade. Neste trabalho, um protocolo de purificação foi desenvolvido, produzindo a enzima na forma homogênea em quantidades suficientes para realizar a caracterização bioquímica da mesma. A enzima necessita de um íon metálico divalente no sítio para catalisar a reação. Suas constantes cinéticas foram determinadas, assim como o mecanismo, os perfis de pH, e a interação com os substratos e produtos através de calorimetria de titulação isotérmica. Um modelo tridimensional da sua estrutura foi construído por homologia de sequência, permitindo uma análise da interação dos substratos e do metal no sítio ativo da enzima. Os resultados obtidos permitirão o desenho racional de moléculas que atuem como inibidores.

ABSTRACT

In 2009, tuberculosis (TB) was responsible for 1.3 million deaths worldwide. The incidence rates reached 9.4 millions and the World Health Organization (WHO) estimative indicates that one third of the world population is infected by *Mycobacterium tuberculosis*, the main agent responsible for the disease. The lack of new drugs released on market, the long period treatment presenting side effects (causing the abandon by the patients) and the cases with HIV co-infection contributed to the appearance of multi drug resistant strains (MDR-TB) and extensively drug resistant strains (XDR-TB). It's clear, thus, that the development of new drugs to fight TB is necessary and fundamental to the success in eradicating this disease. The histidine biosynthesis pathway emerge in this context offering attractive targets, given that its present in prokaryotes, lower eukaryotes and plants, but absent in animals. The last enzyme in the route is called Histidinol Dehydrogenase and is responsible for the conversion of L-Histidinol into L-Histidine. Its essentiality to the bacilli was confirmed by gene knockout, confirming its potential for the development of inhibitory compounds. In this work, a purification protocol was developed, producing the enzyme in the homogeneous form in quantities sufficient to carry its biochemical characterization. The enzyme needs a divalent metal ion in the active site to catalyze the reaction. The kinetic constants were determined, as well as the mechanism, the pH rate profiles and the interaction of its substrates and products by isothermal titration calorimetry. A tridimensional model for its structure was constructed by sequence homology, allowing the analysis of the interaction of the substrates and metal in the active site. The results obtained will allow the rational design of molecules that act as inhibitors.

Capítulo 01

1. Introdução

1.1 A tuberculose

1.2 O *Mycobacterium tuberculosis*

1.3 Resistência a múltiplas drogas

1.4 Biossíntese de histidina e *hisD*

1. INTRODUÇÃO

A tuberculose (TB), causada principalmente pelo *Mycobacterium tuberculosis*, é uma doença infecto-contagiosa com relatos já no Egito e Roma Antigos (DUCATI *et al.*, 2006; PALOMINO *et al.*, 2007). As primeiras lesões típicas da doença, encontradas em múmias egípcias e andinas como deformidades na espinha, datam de até 5 mil anos atrás (BLOOM e MURRAY, 1992). A identificação de material genético do bacilo em tecidos de mamíferos primitivos sugere que a TB é uma doença antiga com ampla distribuição geográfica. A doença foi disseminada no Egito e Roma, existiu na América antes de Colombo e em Bornéu, antes de qualquer contato com o povo europeu. A presença de ácido desoxirribonucléico (DNA) da espécie *M. bovis*, que geralmente infecta animais, também foi encontrada em esqueletos humanos com evidências de TB, sugerindo que os animais com os quais a população estava em constante contato podem ter sido reservatórios para a infecção em humanos (PALOMINO *et al.*, 2007).

A epidemia de TB na Europa iniciou, provavelmente, no começo do século XVII e se estendeu pelos 200 anos seguintes. Cidades da Europa e da América do Norte, após a Revolução Industrial, proporcionavam um ambiente favorável à disseminação do patógeno por via aérea, uma vez que a densidade populacional era alta e as condições sanitárias precárias. Devido a este cenário, durante toda história, a TB foi a principal causa de morte nessas regiões (BLOOM e MURRAY, 1992; PALOMINO *et al.*, 2007). A epidemia se disseminou lentamente para diferentes locais, incluindo a África, devido à exploração e colonização pelos Europeus e Norte-Americanos (PALOMINO *et al.*, 2007).

1.1. A tuberculose

Dentre as doenças infecciosas que já acompanharam o homem ao longo da história, a tuberculose é atualmente a responsável pelo maior número de mortes no mundo. Epidemiologistas estimam que um terço da população mundial esteja infectada pelo bacilo causador da tuberculose, dentro do qual

aproximadamente 8 a 10 milhões de pessoas desenvolvem a doença e 2 milhões morrem anualmente (ENARSON e MURRAY, 1996 PIETERS, 2008; YEW E LEUNG, 2008).

Esta doença vem ressurgindo com força nas últimas décadas, principalmente em países em desenvolvimento, onde se concentram aproximadamente 95% dos casos. Em 1998, o Brasil já ocupava o décimo terceiro lugar entre os 22 países que concentram cerca de 80% dos casos diagnosticados (RUFFINO-NETO, 2002). Hoje segundo dados da Organização Mundial da Saúde (OMS) o Brasil ocupa o décimo nono lugar em termos de casos incidentes (WHO report 2010). Um retrato do quadro global da tuberculose pode ser visto na Figura 1. O ressurgimento da tuberculose tem sido justificado por fatores como a reativação de infecções latentes, a migração de estrangeiros oriundos de países com alta prevalência da doença, casos de co-infecção com o vírus da imunodeficiência humana (HIV), além da transmissão da doença por pessoas com tuberculose ativa (BRENNAN, 1997). Ainda, fatores como a síndrome da imunodeficiência adquirida (AIDS), conglomerados de pessoas em prisões, hospitais e casas de abrigo, e a deterioração do sistema de saúde, entre outros, podem favorecer um aumento da transmissão e, consequentemente, do número de infectados pela doença (RUFFINO-NETO, 2002; BRENNAN, 1997; FATKENHEUER *et al.*, 1999).

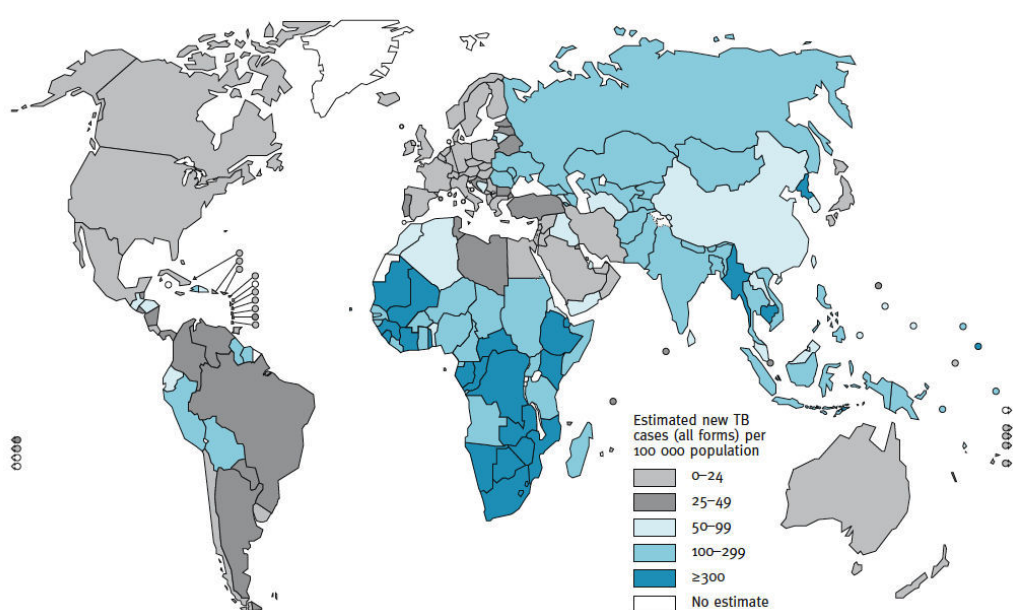


Figura 1. Quadro global da tuberculose: taxas de incidência por país (extraído de: WHO Report 2010, Global Tuberculosis Report).

Esta doença foi introduzida no Brasil pelos portugueses e missionários jesuítas a partir de 1500. Oswaldo Cruz, no início do século 20, procurou implantar planos de ação para combatê-la, ainda que sem obter muito sucesso. Em 1927, Arlindo de Assis aplicou pela primeira vez a vacina oral em crianças recém-nascidas. O uso de agentes tuberculostáticos, como estreptomicina, ácido para-amino-salicílico e isoniazida, a partir da década de 40, reduziu consideravelmente a mortalidade pela tuberculose. Recentemente, a OMS declarou esta doença como urgência de saúde pública global e, em 1996, no Brasil, um plano emergencial foi criado buscando implantar atividades específicas nos locais onde se concentrava a maior parte de casos da doença. Entretanto, a situação ainda não foi completamente controlada, e há um alto índice de casos distribuídos ao longo do país, concentrados principalmente nos estados de São Paulo, Rio de Janeiro, Bahia, Minas Gerais e Rio Grande do Sul (RUFFINO-NETO, 2002).

A primeira descrição formal da capacidade de infecção da tuberculose foi realizada em 1865, pelo cirurgião militar francês Antoine Villemin. Em 1882, o cientista Robert Koch isolou e cultivou o bacilo causador da tuberculose, que, desde então, passou a ser conhecido por Bacilo de Koch. Vinte e seis anos mais tarde, dois pesquisadores do Instituto Pasteur, Albert Calmette e Camille Guérin, cresceram o bacilo bovino, *Mycobacterium bovis*, e observaram que, ao longo das gerações, o bacilo se tornava não virulento quando administrado em modelos animais, abrindo margem para a sua utilização profilática contra a cepa virulenta causadora da tuberculose em humanos. Posteriormente, criou-se uma vacina, chamada de BCG, que é atualmente a mais utilizada em todo mundo (BLOOM e MURRAY, 1992). No entanto, estudos demonstram que a vacina possui uma eficácia que varia entre 0 a 80% em diferentes populações humanas (BRENNAN, 1997).

O diagnóstico da doença pode ser feito através de um teste de reatividade a um derivado purificado de uma proteína do bacilo, a tuberculina, conhecido como PPD, bem como através de exames de raios X torácicos. A detecção do

bacilo também pode ser feita através de baciloscopia, que pode ser realizada de 2 a 8 semanas após a infecção. Métodos de diagnóstico da tuberculose através de teste de PCR e PCR em tempo real, empregando a identificação de seqüências de DNA específicas ao agente etiológico da doença, vêm sendo desenvolvidos, visando maior sensibilidade e especificidade em relação aos métodos diagnósticos atualmente em uso na clínica (BLOOM e MURRAY, 1992; CAWS e DROBNIEWSKI, 2001).

A tuberculose humana é caracterizada por sintomas como fraqueza, febre, dores peitorais, perda de peso, insuficiência respiratória, tosse e escarro hemoptóico. A principal forma de transmissão da tuberculose ocorre através da respiração, uma vez que o bacilo é capaz de se disseminar pelo ar. O desenvolvimento da tuberculose ativa em pessoas infectadas ocorre preferencialmente em situações de supressão do sistema imune, comuns principalmente no decorrer da infecção pelo HIV.

O tratamento para a tuberculose é de difícil manejo, já que requer um longo período de administração de fármacos. Os sintomas da doença desaparecem após 2 a 4 semanas de tratamento contínuo; o que leva muitos pacientes a desistência, já que as drogas utilizadas são consideravelmente tóxicas, apresentando diversos efeitos colaterais e interações medicamentosas. Assim, se criam condições para a seleção de microrganismos resistentes às drogas utilizadas, uma vez que muitos desses pacientes acabam tendo que retomar o tratamento quando este for novamente indicado. Um novo regime terapêutico preconizado pela OMS, conhecido como DOTS tem sido incentivado; neste, se dá a participação de agentes de saúde que acompanham o tratamento dos pacientes, monitorando a administração regular de pelo menos três agentes quimioterápicos e a manutenção do tratamento por um período de 6 a 9 meses. O regime de tratamento consiste na administração de rifampicina, pirazinamida, isoniazida e estreptomicina ou etambutol durante os dois primeiros meses e isoniazida e rifampicina durante mais quatro meses.

1.2. O *Mycobacterium tuberculosis*

O *Mycobacterium tuberculosis*, o agente etiológico da tuberculose humana, apresenta crescimento lento, envelope celular complexo, patogenicidade intracelular e homogeneidade genética. É uma bactéria aeróbia, fracamente Gram-positiva, possuindo entre 0,3 e 0,6 µm de largura e 1 a 4 µm de altura. Esta bactéria infecta e se prolifera no interior de macrófagos, sendo, portanto, um microrganismo intracelular obrigatório (COLE *et al.*, 1998). O gênero é considerado bacilo álcool-ácido resistente (BAAR) devido à capacidade de reter fucsina básica na parede celular mesmo na presença de álcool e ácido, quando para sua coloração é utilizado o método de Ziehl-Neelsen.

A parede micobacteriana possui características incomuns, apresentando uma camada de peptideoglicano composta de ácido N-glicolilmurâmico ao invés de ácido N-acetilmurâmico, comum às demais bactérias. Aproximadamente 60% do envelope celular é composto por ácidos graxos incomuns, conhecidos como ácidos micólicos. Lipídeos livres encontrados na parede celular micobacteriana e que não se encontram ligados aos peptideoglicanos são capazes de atuar de forma antigênica no hospedeiro infectado (BRENNAN e NIKAIDO, 1995). Esta constituição incomum da parede celular facilita sua sobrevivência dentro de macrófagos.

As espécies pertencentes ao gênero *Mycobacterium* compartilham, em geral, muitas características em comum, como a produção de ácidos micólicos na parede celular e uma grande porção do genoma composta por ácidos guanidínicos e citidínicos. O genoma da linhagem melhor caracterizada, o *M. tuberculosis* H37Rv, possui 4.411.529 pares de base dispostos em um cromossomo circular, sendo 65,6% composto por bases G+C (COLE *et al.*, 1998). Esta linhagem tem sido utilizada mundialmente na pesquisa biomédica devido à manutenção de virulência e alta sensibilidade à drogas. Sabe-se que grande parte do genoma de *M. tuberculosis* é responsável pela codificação e produção de enzimas envolvidas em lipólise e lipogênese, e, a partir da análise deste, foi possível identificar o potencial que o bacilo da tuberculose possui na síntese de todos os aminoácidos essenciais, enzimas e vitaminas. O bacilo da tuberculose é naturalmente resistente a muitos antibióticos, devido em parte ao envelope celular hidrofóbico que age como barreira permeável, e em parte à resistência codificada

em seu genoma, que produz enzimas hidrolíticas e modificadoras de drogas. Fosfolipases C, esterases e lipases podem atuar como fatores de virulência, podendo atacar membranas celulares ou vacuolares (COLE *et al.*, 1998).

1.3. Resistência a Múltiplas Drogas

O aparecimento de novas linhagens de *M. tuberculosis* resistentes às drogas utilizadas está se tornando um problema sério e crescente; o tratamento de pacientes infectados com MDR-TB é mais difícil e oneroso, levando à morte do paciente em 80% dos casos. A resistência a múltiplas drogas representa uma preocupação mundial, predominando em países pobres e em desenvolvimento, onde os programas de controle da doença são extremamente ineficientes. O aumento nos casos de resistência se deve principalmente à administração inadequada de medicamentos. A quimioterapia contra a tuberculose se desenvolveu ao final da década de 40, com a utilização de estreptomicina, seguida por ácido para-amino-salicílico (pouco utilizado atualmente) e isoniazida; rifampicina foi introduzida ao final da década de 60, e pirazinamida, já conhecida no final da década de 50, foi introduzida no tratamento contra tuberculose cerca de uma década depois.

A aquisição de resistência de *M. tuberculosis* a múltiplas drogas deve-se a diferentes eventos de mutação cromossômica. Durante a exposição bacteriana aos medicamentos, ocorre uma pressão seletiva a favor de mutantes resistentes. Mecanismos moleculares de resistência em *M. tuberculosis* a agentes antimicobacterianos têm sido evidenciados nos últimos anos; para cada uma das drogas utilizadas, há pelo menos um gene envolvido, ao longo do qual a ocorrência de mutações específicas pode levar ao surgimento de um fenótipo resistente (ZHANG e YOUNG, 1993; PETRINI e HOFFNER, 1999; TELENTI e ISEMAN, 2000).

Pacientes com MDR-TB devem ser tratados com uma combinação de drogas de segunda linha que, além de serem significativamente mais caras, possuem mais efeitos tóxicos e são menos efetivas que as drogas de primeira linha (O'BRIEN e NUNN, 2001). Em países industrializados, o tratamento habitual

custa em torno de 2.000 dólares por paciente, mas alcança 250.000 dólares para pacientes com MDR-TB (PASQUALOTO e FERREIRA, 2001).

Casos de co-infecção de HIV e MDR-TB alcançam taxas de mortalidade próximas a 100%, e esta é definida como a infecção oportunista mais maligna associada à AIDS (FÄTKENHEUER et al., 1999). Cerca de 300.000 novos casos de MDR-TB são diagnosticados a cada ano, sendo que de 4 a 20 % destes são classificados como TB extensivamente resistente (XDR-TB), definida como casos de TB cujos isolados são resistentes à isoniazida, rifampicina e a pelo menos três das seis principais classes de drogas de segunda linha (aminoglicosídeos, polipetídeos, fluoroquinolonas, tiamidas, cicloserina e ácido p-aminosalicílico) (DORMAN e CHAISSON, 2007; CDC, 2006). XDR-TB está sendo relatada em todo o mundo, inclusive nos Estados Unidos, onde a TB estava sendo considerada sob controle. A ocorrência já difundida de XDR-TB traz discussões sobre a drástica situação de casos de TB virtualmente incuráveis e aponta para a urgente necessidade de introduzir novos e eficazes fármacos anti-TB (DORMAN e CHAISSON, 2007).

A elucidação dos mecanismos moleculares que levam à formação de linhagens resistentes às drogas utilizadas será de grande utilidade para o desenvolvimento de novas ferramentas e novos tratamentos a pacientes infectados com bacilos resistentes. Dessa forma, a pesquisa para o desenvolvimento de novos agentes antimicobacterianos torna-se necessária, bem como a identificação de novos alvos para futuros medicamentos. A otimização de vacinas de ação profilática ou terapêutica, de forma a atuar especificamente contra o bacilo causador da tuberculose também deve ser considerada para o desenvolvimento de uma estratégia eficaz para reduzir significativamente o número de casos de tuberculose.

1.4. Biossíntese de Histidina e *hisD*

A via de biossíntese de histidina, presente nos organismos procarióticos, em organismos eucarióticos inferiores e em plantas, é ausente em animais. Em função disto, as enzimas que a compõe geram grande interesse como potenciais

alvos para a ação de novas drogas antimicrobianas e herbicidas. Os organismos que apresentam esta via são capazes de converter fosforibosil pirofosfato (PRPP) e ATP em histidina, por meio de dez passos enzimáticos (Figura 2).

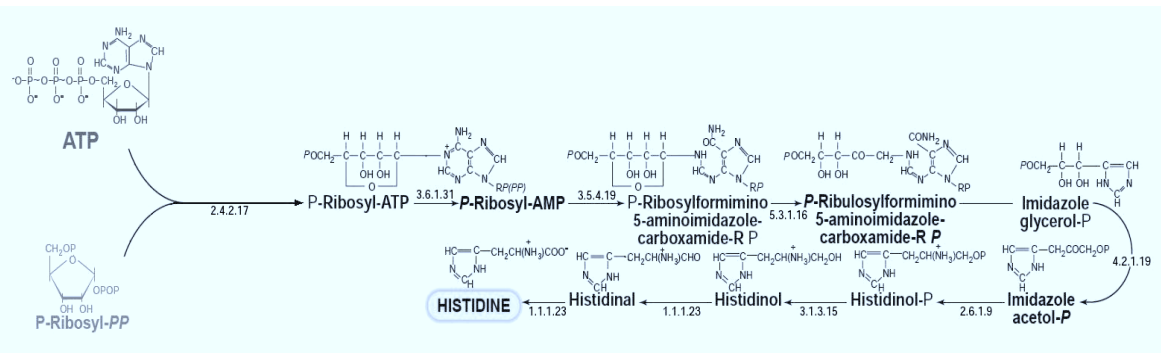


Figura 2. Via de biossíntese de histidina. Partindo dos precursores ATP e PRPP, em dez etapas catalisadas por enzimas ocorre a produção de histidina. A enzima histidinol desidrogenase é responsável pelas duas últimas reações.

A primeira enzima da rota é o produto do gene *hisG*, responsável pela condensação de PRPP e ATP em N'-5'-Fosforibosil-ATP e é chamada de N'-5'-Fosforibosil-ATP Transferase (E.C. 2.4.2.17) (ALIFANO *et al.*, 1996). A próxima etapa da via é a hidrólise irreversível do N'-5'-Fosforibosil-ATP para N'-5'-Fosforibosil-AMP, uma das duas atividades correspondentes a enzima codificada pelo gene *hisI* (E.C. 3.6.1.31). A seguir, a mesma enzima faz o papel de ciclohidrolase (E.C. 3.5.4.19), abrindo o anel purínico do N'-5'-Fosforibosil-AMP, levando a formação da aminoaldeído N'-[(5'-Fosforibosil)-Formoimino]-5-aminoimidazol-4-carboxamida-ribonucleotídeo. O quarto passo da rota é uma reação redox interna à molécula, isomerizando a aminoaldeído a uma aminocetose (N'-[(5'-Fosforibulosil)-formimino]-5-aminoimidazol-carboxamida-ribonucleotídeo) catalisada pelo produto do gene *hisA* (E.C. 5.3.1.16). Seguindo a rota, os produtos dos genes *hisH* e *hisF* formam um heterodímero (também chamado de IGP sintase) para catalisar a conversão da aminocetose em Imidazol-Glicerol-Fosfato (IGP) e 5'-fosphoribosil-4-carboxamide-5-aminoimidazol (AICAR). Nesse ponto a via de biossíntese de histidina e a via de síntese *de novo* de purinas se interligam, pois o AICAR pertence a ambas as vias. O IGP é então desidratado (E.C. 4.2.1.19) por outra enzima bifuncional pertencente à rota (codificada pelo gene *hisB*), produzindo Imidazol-Acetol-Fosfato (IAP). A sétima etapa da via é

levada pela aminotransferase codificada pelo gene *hisC* (E.C. 2.6.1.9), transformando o IAP em L-Histidinol-Fosfato (L-Hol-P). A atividade de fosfatase (E.C. 3.1.3.15) da enzima codificada pelo gene *hisB* transforma o L-Hol-P em L-Histidinol (L-Hol). Finalmente, as duas últimas etapas são catalisadas pela enzima Histidinol Desidrogenase (E.C. 1.1.1.23), convertendo L-Hol no intermediário L-Histidinal e encerrando a via com o produto L-Histidina (Figura 3) (VOET, 2004).

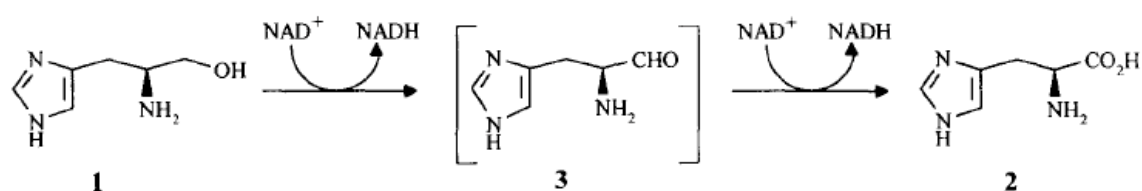


Figura 3: Reação catalisada pela enzima Histidinol Desidrogenase. 1: L-Histidinol, 2: L-Histidina, 3: L-Histidinal (intermediário).

O sequenciamento completo do genoma do *M. tuberculosis* identificou 3.924 ORFs, que poderão, por sua vez, auxiliar no desenvolvimento de métodos profiláticos e terapêuticos de combate ao patógeno (COLE *et al.*, 1998). Estratégias baseadas no desenho de novas drogas dependem da identificação de rotas bioquímicas específicas ao microorganismo, onde muitas delas já foram caracterizadas a nível genético. A identificação de genes envolvidos na codificação das enzimas que compõem estas vias metabólicas e a utilização destes através de técnicas de DNA recombinante propicia uma caracterização estrutural e funcional mais detalhada de potenciais alvos moleculares para o desenvolvimento de inibidores de ação seletiva.

Estudos recentes de mutagênese demonstraram que os genes da via de biossíntese de histidina são essenciais para a sobrevivência do *M. tuberculosis*; organismos auxotróficos para histidina não resistem à restrição deste aminoácido (PARISH, 2003; SASSETTI, 2003). Ainda mais específico foi o estudo que demonstrou a essencialidade do gene *hisD* em mutantes de *M. tuberculosis* com o referido gene inactivado, produzidos por recombinação homóloga (PARISH *et al.*, 1999).

A partir da elucidação de todas estas informações, e da identificação da ORF Rv1599 em *M. tuberculosis* H37Rv como o provável gene codificante para histidinol desidrogenase micobacteriana (438 aminoácidos, 45.346,10 Da) (COLE *et al.*, 1998), podemos afirmar que esta enzima representa um potencial candidato a alvo para o desenvolvimento de novas drogas contra a tuberculose. Concordante, a enzima foi apontada entre os 50 melhores alvos para desenvolvimento de drogas contra tuberculose pelo banco de dados TDR Targets (AGUERO *et al.*, 2008).

Fica claro, portanto, a necessidade de se produzir a enzima de maneira homogênea que venha a possibilitar o estudo de sua atividade, fazendo-se entender a sua interação com seus substratos, seu mecanismo e modo de ação. Ainda, a determinação da estrutura tridimensional da enzima histidinol desidrogenase de *E. coli* por difração de raios X (BARBOSA *et al.*, 2002) pode auxiliar na futura modelagem molecular de tal enzima micobacteriana. A disponibilidade da estrutura da enzima histidinol desidrogenase de *M. tuberculosis* viabilizará o desenho de inibidores específicos, baseados no detalhado modelo do sítio de ligação da enzima aos seus substratos.

Anteriormente em nosso grupo de pesquisa, o gene *hisD* de *M. tuberculosis* H37Rv foi amplificado a partir de DNA genômico do bacilo, clonado em vetor de expressão pET23a(+) e sequenciado para confirmação de sua integridade. Testes de expressão foram realizados onde a enzima foi encontrada na fração solúvel da cepa BL21(DE3) de *E. coli* quando cultivada por 18h em meio LB à 37°C sem indução por IPTG. Estes dados e materiais produzidos serviram como base para o presente projeto.

Capítulo 02

2. Objetivos

2.1 Objetivo Geral

2.2 Objetivos Específicos

2. OBJETIVOS

Na busca pelo desenvolvimento de alternativas para o tratamento da TB, este trabalho se pauta no alvo apresentado, a fim de se gerar resultados para auxiliar no cunho de novos fármacos efetivos contra a doença.

2.1. Objetivo Geral

A determinação de um protocolo de purificação e estudos de cinética enzimática para a caracterização da enzima Histidinol Desidrogenase de *Mycobacterium tuberculosis* são o alvo deste trabalho que servirá como base para o entendimento do funcionamento da enzima permitindo o desenho racional de novas drogas contra a tuberculose.

2.2. Objetivos Específicos

- I. Estabelecer um protocolo de purificação para a enzima Histidinol Desidrogenase;
- II. Determinar o peso molecular em solução bem como da subunidade;
- III. Comprovar a hipótese de que a enzima Histidinol Desidrogenase de *Mycobacterium tuberculosis* é uma metaloenzima, estudando sua interação com metais divalentes;
- IV. Realizar o estudo de perfis de pH para entender o papel da catálise ácido/base no mecanismo da enzima;
- V. Determinar as constantes cinéticas verdadeiras em estado estacionário;
- VI. Estudar a ligação dos substratos e produtos com a enzima por meio de calorimetria de titulação isotérmica (ITC);
- VII. Determinar o mecanismo cinético da enzima;
- VIII. Criar um modelo para a estrutura tridimensional da proteína baseado na estrutura de *E. coli* através de modelagem comparativa por homologia.

Capítulo 03

Artigo publicado no Archives of Biochemistry and Biophysics – Molecular, kinetic, thermodynamic, and structural analyses of *Mycobacterium tuberculosis* *hisD*-encoded metal-dependent dimeric histidinol dehydrogenase (EC 1.1.1.23)



Molecular, kinetic, thermodynamic, and structural analyses of *Mycobacterium tuberculosis* *hisD*-encoded metal-dependent dimeric histidinol dehydrogenase (EC 1.1.1.23)

José E.S. Nunes ^{a,b}, Rodrigo G. Ducati ^a, Ardala Breda ^{a,b}, Leonardo A. Rosado ^{a,b}, Bibiana M. de Souza ^c, Mario S. Palma ^c, Diógenes S. Santos ^{a,b,*}, Luiz A. Basso ^{a,b,*}

^a Centro de Pesquisas em Biologia Molecular e Funcional (CPBMF), Instituto Nacional de Ciência e Tecnologia em Tuberculose (INCT-TB), Pontifícia Universidade Católica do Rio Grande do Sul (PUCRS), Av. Ipiranga 6681, Porto Alegre 90619-900, RS, Brazil

^b Programa de Pós-Graduação em Biologia Celular e Molecular, PUCRS, Porto Alegre, RS, Brazil

^c Instituto de Biociências de Rio Claro, Universidade Estadual Paulista (UNESP), Avenida 24A, 1515, Rio Claro, SP 13506-900, Brazil

ARTICLE INFO

Article history:

Received 16 March 2011
and in revised form 26 May 2011
Available online 6 June 2011

Keywords:

Histidinol dehydrogenase
Mycobacterium tuberculosis
Metalloenzyme
Thermodynamic binding parameters
Enzyme mechanism
Molecular model

ABSTRACT

The emergence of drug-resistant strains of *Mycobacterium tuberculosis*, the major causative agent of tuberculosis (TB), and the deadly HIV-TB co-infection have led to an urgent need for the development of new anti-TB drugs. The histidine biosynthetic pathway is present in bacteria, archaea, lower eukaryotes and plants, but is absent in mammals. Disruption of the *hisD* gene has been shown to be essential for *M. tuberculosis* survival. Here we present cloning, expression and purification of recombinant *hisD*-encoded histidinol dehydrogenase (*MtHisD*). N-terminal amino acid sequencing and electrospray ionization mass spectrometry analyses confirmed the identity of homogeneous *MtHisD*. Analytical gel filtration, metal requirement analysis, steady-state kinetics and isothermal titration calorimetry data showed that homodimeric *MtHisD* is a metalloprotein that follows a Bi Uni Uni Bi Ping-Pong mechanism. pH-rate profiles and a three-dimensional model of *MtHisD* allowed proposal of amino acid residues involved in either catalysis or substrate(s) binding.

© 2011 Elsevier Inc. All rights reserved.

Introduction

The World Health Organization (WHO) declared tuberculosis (TB)¹ as a global emergency in 1993. Unfortunately, the efforts made by the Stop TB Strategy were not enough to impede the occurrence of 1.3 million deaths in 2009 [1]. However, WHO estimates that the number of cases per capita peaked at 2004 and is slowly falling [2]. Nonetheless, the battle against TB is far from over, since *Mycobacterium tuberculosis* (the main causative agent of TB) proved to be highly adaptive [3] and capable of evading the current strategies for treatment of 0.5 million cases of multi-

drug-resistant TB (MDR-TB) that were reported in 2007, including cases of extensively drug-resistant TB (XDR-TB) [2], and the more recently reported totally drug-resistant strains (TDR-TB) [4,5]. To compound the problem further, the deadly association with human immunodeficiency virus makes the treatment of co-infected patients even more challenging [2]. Accordingly, novel TB treatments should, hopefully, reduce the duration of short-course treatment, lower the dose frequency, reduce the pill burden, and prevent low drug-drug interactions [6].

The histidine biosynthetic pathway has been studied in detail in *Salmonella typhimurium* and *Escherichia coli*. There are 10 enzymatic reactions carried out by eight gene products in the unbranched pathway that include several complex and unusual reactions, and form a critical link between amino acid and purine biosynthesis [7]. The final reaction, first described in *Arthrobacter histidinovorans* and *E. coli* [8], and in yeast [9], is catalyzed by histidinol dehydrogenase (HisD) [*L*-histidinol:NAD oxidoreductase (EC 1.1.1.23)]. HisD is a bifunctional enzyme that catalyzes the NAD⁺- and Zn²⁺-dependent conversion of *L*-histidinol (*L*-Hol) to *L*-histidine (*L*-His) through an *L*-histidinaldehyde (*L*-Hal) intermediate [8–10], with the concomitant reduction of 2 mol of NAD⁺ (Fig. 1A). Previously described HisD enzymes are homodimers [11,12] containing one Zn²⁺ per subunit [11]; and they are

* Corresponding authors at: Av. Ipiranga 6681, Tecnopuc, Prédio 92A, Porto Alegre 90619-900, RS, Brazil. Fax: +55 51 33203629.

E-mail addresses: diogenes@pucrs.br (D.S. Santos), luiz.basso@pucrs.br (L.A. Basso).

¹ Abbreviations used: DMSO, dimethyl sulfoxide; DOTS, directly observed treatment short-course; ESI-MS, electrospray ionization mass spectrometry; HisD, histidinol dehydrogenase; IPTG, isopropyl β-D-thiogalactopyranoside; ITC, isothermal titration calorimetry; LB, Luria-Bertani; *L*-Hol, *L*-histidinol; *L*-Hal, *L*-histidinaldehyde; *L*-His, *L*-histidine; MDR, multidrug-resistant; MtHisD, *Mycobacterium tuberculosis* HisD; MWCO, molecular weight cut off; NAD⁺, nicotinamide adenine dinucleotide, oxidized form; NADH, nicotinamide adenine dinucleotide, reduced form; PDB, Protein Data Bank; pl, isoelectric point; RMSD, root-mean square deviation; TB, tuberculosis; WHO, World Health Organization; XDR, extensively drug-resistant.

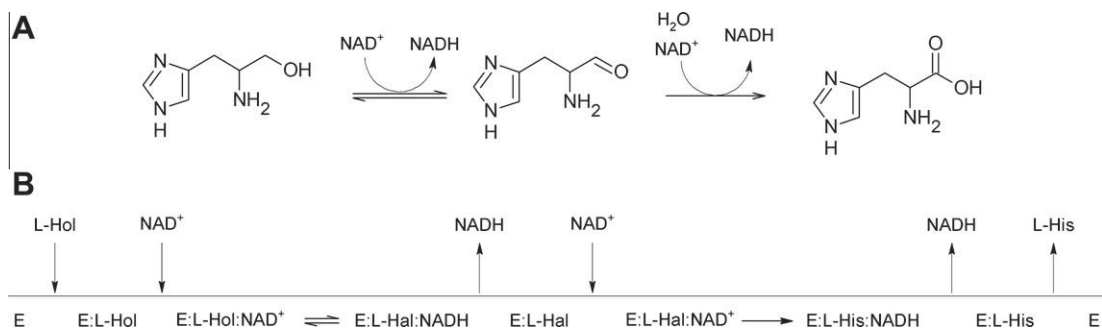


Fig. 1. Chemical reaction catalyzed by HisD. (A) HisD catalyzes the NAD⁺- and Zn²⁺-dependent conversion of L-Hol to L-His through an L-Hal intermediate, with the concomitant reduction of 2 mol of NAD⁺. (B) Proposed Bi Uni Uni Bi Ping-Pong enzyme mechanism for MtHisD-catalyzed chemical reaction.

therefore examples of metalloenzymes. Interestingly, it has been pointed out that relatively few other NAD⁺-linked oxidoreductases seem to require a bound metal for activity [13].

The histidine biosynthetic pathway is present in bacteria, archaeabacteria, lower eukaryotes and plants, but is absent in mammals [14]. Analysis of the complete genome sequence of *M. tuberculosis* H37Rv strain predicted the presence of the coding sequences for the histidine biosynthetic pathway enzymes [15]. The inability of histidine auxotrophs to survive single-amino-acid starvation [16], the identification of genes required for mycobacterial growth [17], and the essentiality of the *hisD* gene product for *M. tuberculosis* survival [18] suggest that HisD is a promising target for antitubercular agent development. Not surprisingly, HisD has been ranked among the top 50 targets by the TDR Targets database [19]. However, it has not been shown yet whether the *hisD* gene codes for a histidinol dehydrogenase activity as predicted by *in silico* analysis of *M. tuberculosis* genome sequence.

The target-based rational design of new agents with anti-TB activity includes functional and structural efforts. However, the first step to enzyme target validation must include experimental data demonstrating that a gene predicted by *in silico* analysis to encode a particular protein catalyzes the proposed chemical reaction. Moreover, recognition of the limitations of high-throughput screening approaches in the discovery of candidate drugs has rekindled interest in rational design methods. Understanding the mode of action of MtHisD should thus inform us on how to better design inhibitors targeting this enzyme with potential therapeutic application in TB chemotherapy.

Here we present cloning, expression, purification to homogeneity, steady-state kinetics, pH-rate profiles, metal requirement studies, isothermal titration calorimetry data on ligand binding, and molecular homology model building of MtHisD. These data prompted the proposal that MtHisD follows a Bi Uni Uni Bi Ping-Pong mechanism. In addition, these studies indicated the likely amino acid residues involved in acid-base catalysis and/or substrate binding. These studies should provide a framework on which to base the rational design of MtHisD enzyme inhibitors to be tested as antiTB agents.

Materials and methods

PCR amplification, cloning and overexpression of recombinant *M. tuberculosis* hisD-encoded protein

Synthetic oligonucleotide primers (5'-c**catat**gcttaccgcgtatcgac-ttgccggag-3' and 5'-t**caagg**tgtatcgctcgaaacctccgcgtac-3') were designed to be complementary to, respectively, the amino-terminal coding and carboxy-terminal noncoding strands of *hisD* (*Rv1599* locus) gene containing 5' *NdeI* and 3' *HindIII* restriction sites (in bold), and the start and stop codons (in italics). These

primers were used to amplify the *M. tuberculosis* *hisD* structural gene (1317 bp) from genomic DNA using standard PCR conditions (Perkin-Elmer) with a hot start at 99 °C for 10 min. The amplified fragment was purified with CONCERT Nucleic Acid Purification System (Gibco BRL), digested with *NdeI* (Invitrogen) and *HindIII* (Gibco BRL), and ligated into a pET-23a(+) expression vector (Novagen). The DNA sequence of the *M. tuberculosis* *hisD* structural gene was determined using an ABI-PRISM 3100 Genetic Analyzer (Applied Biosystems) to both confirm the identity of the cloned DNA and ensure that no mutations were introduced by the PCR amplification step.

Overexpression was achieved by transforming electrocompetent *E. coli* BL21(DE3) host cells with pET-23a(+)::*hisD* recombinant plasmid and grown on Luria-Bertani (LB) medium containing 50 µg mL⁻¹ carbenicillin at 37 °C for 18 h after reaching OD_{600nm} = 0.4 without induction by isopropyl β-D-thiogalactopyranoside (IPTG). Cells were harvested by centrifugation at 12,000g for 15 min at 4 °C, and stored at -20 °C.

Protein purification

Approximately 9 g of wet cell paste were suspended in 45 mL of 100 mM Pipes pH 6.0 (buffer A), treated with lysozyme 0.2 mg mL⁻¹ at 4 °C for 30 min with gentle stirring, disrupted by sonication with 8 pulses of 15 s each at 60% amplitude with a 13 mm probe. This solution was centrifuged at 48,000g for 30 min at 4 °C, and 10 mM MgCl₂ (final concentration) and 2000 units of bovine pancreas DNase I (Sigma) were added to the soluble fraction (~40 U mL⁻¹) under gentle stirring at 4 °C for nucleic acid removal. This mixture was centrifuged at 48,000g at 4 °C for 30 min and the supernatant dialyzed against buffer A before being loaded on a Q Sepharose Fast Flow 26/10 (GE Healthcare) column using an Äkta Purifier (GE Healthcare). The column was washed with 4 bed volumes of buffer A and adsorbed protein elution was carried out using a linear gradient of 0–0.5 M NaCl in buffer A. The recombinant *M. tuberculosis* histidinol dehydrogenase (MtHisD) protein eluted at approximately 200 mM NaCl concentration. Fractions were pooled and concentrated using an ultrafiltration membrane with 30 kDa molecular weight cut off (MWCO) and loaded on a HiLoad Superdex 200 26/60 (GE Healthcare) pre-equilibrated with 100 mM Pipes pH 7.2 (buffer B) at 0.8 mL min⁻¹. Fractions containing MtHisD were pooled and loaded on a Mono Q HR 16/10 column (GE Healthcare) equilibrated with buffer B. The column was washed with 2 bed volumes of buffer B and adsorbed protein eluted with a linear 0–0.3 M NaCl gradient in buffer B. Fractions containing homogeneous recombinant MtHisD were dialyzed against buffer B, and stored at -80 °C.

Protein concentration was determined by the method of Bradford [20] using the Bio-Rad protein assay kit (Bio-Rad) and bovine serum albumin as standard.

N-terminal amino acid sequencing and mass spectrometry analysis

Automated Edman degradation was performed with homogeneous *MtHisD* using a gas-phase sequencer PPSQ-21 A (Shimadzu) to verify N-terminal amino acid sequence. *MtHisD* was also analyzed by electrospray ionization mass spectrometry (ESI-MS) according to Chassaigne and Lobinski, with some adaptations [21]. The sample was analyzed on Quattro-II triple-quadrupole mass spectrometer (Micromass; Altrincham, UK). During all experiments, the source temperature was maintained at –80 °C and the capillary voltage at 3.6 kV; a drying nitrogen gas flow (200 L h^{−1}) and a nebulizer gas flow (20 L h^{−1}) were used. The mass spectrometer was calibrated with intact horse heart myoglobin and its typical cone voltage-induced fragments. About 50 pmol (10 µl) of each sample was injected into the electrospray transport solvent. The ESI spectrum was obtained in the multichannel acquisition mode, with scanning from 500 to 1800 m/z at a scan time of 7 s. The mass spectrometer is equipped with MassLynx and Transform software for data acquisition and spectrum handling.

Determination of molecular mass and oligomeric state of *MtHisD* in solution

Analytical gel filtration was performed using a Superdex 200 HR 10/30 (GE Healthcare) column pre-equilibrated with 50 mM Tris HCl pH 7.5 containing 200 mM NaCl at a flow rate of 0.4 mL min^{−1}, with UV detection at 215, 254 and 280 nm. Homogeneous recombinant *MtHisD* was previously dialyzed against the same buffer. The LMW and HMW Gel Filtration Calibration Kits (GE Healthcare) were used to prepare a calibration curve. The elution volumes (V_e) of standard proteins (ferritin, catalase, aldolase, coalbumin, ovalbumin, ribonuclease A) were used to calculate their corresponding partition coefficient (K_{av} , Eq. (1)). Blue dextran 2000 (GE Healthcare) was used to determine the void volume (V_0). V_t is the total bead volume of the column. The K_{av} value for each protein was plotted against their corresponding molecular mass.

$$K_{av} = \frac{V_e - V_0}{V_t - V_0} \quad (1)$$

Histidinol dehydrogenase assay

HisD catalyzes the sequential NAD⁺-dependent oxidations of L-Hol to L-Hal and then to L-His. The enzymatic activity was assayed in the forward direction at 25 °C by continuously monitoring the increase in absorbance at 340 nm due to the conversion of NAD⁺ to NADH ($\epsilon_{NADH} = 6.22 \times 10^3 \text{ M}^{-1} \text{ cm}^{-1}$) [22]. One unit of enzyme activity (U) is defined as the amount of enzyme catalyzing the conversion of 1 µmol of substrate per minute. Enzyme inactivation, divalent metal ion activation and determination of steady-state kinetic constants were carried out in 50 mM Pipes pH 7.2. The curves were plotted and steady-state parameters were determined using the nonlinear regression function of Sigma Plot 9.0.

Inactivation by chelating agents

Histidinol dehydrogenases from other organisms have been described as Zn²⁺ metalloenzymes [12,13,23]. In order to investigate whether *MtHisD* belongs to this class, measurements of enzyme activity were carried out in the presence of 0.1, 1 and 10 mM EDTA and 1, 2 and 5 mM 1,10-phenanthroline. All buffers were rendered metal free by treatment with Chelex resin (Bio-Rad).

Divalent metal ion activation

To assess the ability of different divalent metal ions to activate *MtHisD* enzyme activity, homogeneous enzyme was inactivated with 5 mM 1,10-phenanthroline for 5 min and then diluted 10-fold as described by Charles Grubmeyer [13]. After dilution, 10 µL samples were assayed in the presence of Ca²⁺, Cd²⁺, Co²⁺, Mg²⁺, Mn²⁺, Ni²⁺ and Zn²⁺.

Inductively coupled plasma atomic emission spectroscopy (ICP-AES) analysis of metal content

A semi-quantitative analysis was performed to investigate the divalent metals present in the protein sample. A quantitative analysis of Mn²⁺ and Zn²⁺ concentrations in *MtHisD* homogeneous protein solution was carried out by ICP-AES (Spectro Ciros CCD). Recombinant homogeneous *MtHisD* was extensively dialyzed against Pipes 100 mM pH 7.2 and concentrated by ultrafiltration to a final protein concentration of 8 mg mL^{−1} (enzyme subunit concentration = 8 mg mL^{−1}/45378.2 Da = 176.3 µM).

Determination of steady-state kinetic parameters and enzyme mechanism

To determine the true steady-state kinetic constants and initial velocity patterns, *MtHisD* activity was measured in the presence of variable concentrations of L-Hol (10–250 µM) and several fixed-varied concentrations of β-NAD⁺ (1–25 mM). Steady-state parameters were calculated by fitting the initial velocity data to Eq. (2) [24]. This equation describes the velocity equation in the absence of products for a Bi Uni Uni Bi Ping Pong Ter Ter System assuming that [B] = [C] and $K_B = K_C$, in which v is the initial velocity, V_{max} is the maximal initial velocity, A and B are the concentrations of the substrates (L-Hol and β-NAD⁺), K_A and K_B are their respective Michaelis constants, and K_{iA} is the dissociation constant for enzyme-substrate A (*MtHisD*:L-Hol) binary complex formation.

$$V = \frac{V_{max}[A][B]}{K_{iA}K_B + 2K_B[A] + K_A[B] + [A][B]} \quad (2)$$

Isothermal titration calorimetry (ITC) measurements of ligand binding

Isothermal titration calorimetry (ITC) using an iTC₂₀₀ microcalorimeter (Microcal, Inc., Northampton, MA) was performed to assess the enzyme interaction with its substrates and products. ITC measurements were carried out at 25 °C, and titrations were performed using a 39 µL-syringe, with stirring at 500 rpm. Each titration consisted of a preliminary injection of 0.5 µL, followed by 10 injections of 3.85 µL and 180 s intervals between injections, into a cell containing 200 µL of protein sample at 69 µM for substrates and 131 µM for products. Ligand concentrations were 400 µM (L-Hol), 800 µM (L-His) and 50 mM (NAD⁺ or NADH). To account for dilution and mixing effects, control experiments were performed injecting ligand into buffer instead of protein in the cell. The control data were subtracted to obtain accurate values for heat changes. The Gibbs free energy (ΔG) of binding was calculated using the relationship described in Eq. (3), in which R is the gas constant (8.314 J K^{−1} mol^{−1}), T is the temperature in Kelvin (T = °C + 273.15), and K_a is the association constant at equilibrium. The entropy of binding (ΔS) can also be determined from this mathematical formula. One set of sites model was utilized to determine the binding and thermodynamic constants. Estimates for K_a and the binding enthalpy (ΔH) were refined by standard Marquardt nonlinear regression method provided in the Origin 7 SR4 software.

$$\Delta G^\circ = -RT \ln K_a = \Delta H^\circ - T\Delta S^\circ \quad (3)$$

pH-rate profiles

To assess the role of acid/base chemistry in the *MtHisD* enzymatic reaction, apparent steady-state kinetic constants were determined in a composite buffer (100 mM Mes/Hepes/Ches) with pH values ranging from 7.5 to 11.0. The catalytic constants (k_{cat}) and the specificity constants (k_{cat}/K_M) for each substrate were plotted in the logarithm form against pH. The pH-rate profiles were fitted to either Eq. (4) or Eq. (5) [25], in which y is the kinetic parameter (k_{cat} or k_{cat}/K_M), C is the pH-independent value of y , $10^{-\text{pH}}$ is the proton concentration, and K_a and K_b are, respectively, the apparent acid and base dissociation constants for ionizing groups.

$$\log y = \log \left(\frac{C}{1 + \frac{10^{-\text{pH}}}{K_a}} \right) \quad (4)$$

$$\log y = \left(\frac{C}{1 + \frac{K_b}{K_a} + \frac{10^{-\text{pH}}}{K_a} + \frac{K_b}{10^{-\text{pH}}}} \right) \quad (5)$$

Data described in Fig. 5A and B were best fitted to Eq. (4), which describes a pH-rate profile for a group that needs to be unprotonated (slope of +1) for catalysis (k_{cat}) or L-Hol substrate binding (k_{cat}/K_M). Data given in Fig. 5C were best fitted to Eq. (5), which describes a bell-shaped pH-rate profile for a single ionizing group in the acidic limb that must be unprotonated (slope of +1) for NAD^+ binding and participation of a single ionizing group in the basic limb that must be protonated for substrate binding (slope of -1). It should be pointed out that Eq. (5) describes a bell-shaped pH-rate profile in which the two pKs are less than a pH unit apart [25].

Molecular homology model building

The search for templates for the *MtHisD* target sequence was performed with Blastp [26]. The structure of the homologous *E. coli* protein was selected from the Protein Data Bank (PDB) [27], which was solved experimentally by X-ray diffraction at 1.7 Å resolution (PDB ID: 1KAE). Target and template sequence alignment was performed with ClustalW [28] and required small gaps in both *M. tuberculosis* and *E. coli* HisD amino acid sequences (insertions and/or deletions).

MtHisD protein models were built with restrained-based modeling implemented in MODELLER9v1 [29], with the standard protocol of the comparative protein structure modeling methodology, by satisfaction of spatial restraints [30,31]. The best models were selected according to MODELLER objective function [32] and were subject to energy minimization and stereochemical analysis with PROCHECK [33]. Each subunit of *MtHisD* homodimer was modeled independently based on the *E. coli* structure, in which subunit A is in the apo form and subunit B has both substrates, histidinol and NAD^+ , bound to its active site. Atomic coordinates of heteroatom Zn^{2+} present in both subunits were copied from the template structure into the *MtHisD* model. Prior to energy minimization, the homodimeric structure was assembled based on the template structure with LEaP module of AMBER7 package [34].

Energy minimization

Energy minimization of the best models were performed with GROMACS package [35] using the 43a1 force-field. The system was submitted to an initial steepest descent energy minimization in vacuo with a maximum number of 400 minimization steps, followed by a maximum of 3000 steps of conjugate gradient energy minimization. Identities between the final minimized model of *MtHisD* and the template were evaluated by their root-mean

square deviation (RMSD). Figures were prepared with the PyMOL v0.98 graphics package [36].

Results and discussion

Amplification, cloning, expression and purification of recombinant *M. tuberculosis* histidinol dehydrogenase (*MtHisD*)

The probable *hisD* structural gene was PCR amplified from *M. tuberculosis* H37Rv genomic DNA. The presence of 10% DMSO in the reaction mixture proved to be necessary to obtain a PCR product (data not shown). The DMSO cosolvent helps overcome polymerase extension difficulties due to DNA secondary structures and improves the denaturation of GC-rich DNAs [37], which is consistent with the 65.6% G + C content of *M. tuberculosis* genome [15].

The PCR product was cloned into pET-23a(+) expression vector between *Nde*I and *Hind*III restriction sites. Nucleotide sequence analysis of the cloned DNA fragment confirmed the identity of the insert as *M. tuberculosis* *hisD* coding sequence (1317 bp) and demonstrated that no mutations were introduced by the PCR amplification step.

Histidinol dehydrogenase from *M. tuberculosis* H37Rv (*MtHisD*) was overexpressed in *E. coli* BL21(DE3) electrocompetent host cells transformed with pET-23a(+)::*hisD* recombinant plasmid. To evaluate recombinant *MtHisD* expression as a function of time, cell growth was tested for 3, 6, 12, 18, 24, and 48 h at 37 °C either with or without IPTG induction. SDS-PAGE analysis revealed a higher yield of soluble recombinant protein in the absence of IPTG for cells grown for 18 h (data not shown). Interestingly, the recombinant *MtHisD* protein overexpression was achieved with no addition of the inducer. The pET system makes use of a highly processive T7 RNA polymerase under control of the IPTG-inducible *lacUV5* promoter for the transcription of target genes of interest [38]. Reports have demonstrated that high levels of protein production can be obtained in the stationary phase of cell growth in the absence of IPTG induction [39–41]. It has been proposed that leaky protein expression occurs for *lac*-controlled systems when cells approach stationary phase in complex medium and that cyclic AMP, acetate and low pH are required to affect expression in the absence of IPTG induction [42]. However, it has later been shown that unintended induction in the pET system is likely due to the presence of as little as 0.0001% of lactose in the medium [43].

Purification of recombinant *MtHisD* has proved to be, at least in our hands, not a trivial task. A number of protocols were attempted to purify *MtHisD* enzyme to homogeneity with no success, even using a His-tagged construction (data not shown). Incidentally, His-tag purification is not suitable in this case because imidazole, used to elute proteins from affinity columns seems, not surprisingly, to inhibit the enzyme activity. In addition, *MtHisD* is a metal-dependent enzyme (as will be described in the next section) and the fusion of a His-tag to the recombinant protein could confound interpretation of results. Accordingly, we have opted to use a construction without any fused partner. As *MtHisD* has a low theoretical isoelectric point ($\text{pI} = 4.85$), it was deemed advantageous to use a pH value as low as possible to reduce the likelihood of *E. coli* proteins being adsorbed to the anion exchange columns (Q Sepharose Fast Flow and Mono Q). Moreover, different substances have different degrees of interaction with the ion exchanger due to differences in their charges, charge densities and distribution of charge on their surfaces, and these interactions can be controlled by varying conditions such as pH. Hence, *MtHisD* purification protocol employed 100 mM Pipes pH 6.0 buffer for the first Q Sepharose Fast Flow anion exchange column, which resulted in improved recombinant protein yield. Buffer exchange (from buffer A to B) and salt removal were achieved in HiLoad Superdex

Table 1

Typical purification protocol starting from 9 g of cells.

Sample	Total protein (mg)	Total enzyme activity (U)	Specific activity (U mg^{-1})	Purification fold	Yield (%)
Crude extract	693	24	0.03	1.0	100
Q Sepharose	60	28	0.5	17	117
Superdex 200	24	22	0.9	30	92
Mono Q	7.6	10	1.2	40	42

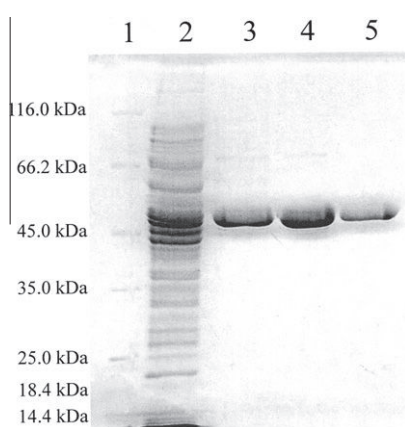


Fig. 2. SDS-PAGE analysis of pooled fractions of desorbed proteins for each purification step. (Lane 1) MW markers (Protein Marker – Fermentas); (Lane 2) crude extract; (Lane 3) Q Sepharose Fast Flow ion exchange; (Lane 4) Superdex 200 gel filtration and (Lane 5) Mono Q ion exchange.

gel filtration column. The third step of the purification protocol employed Mono Q anion exchange column that yielded *MtHisD* in homogeneous form. This *MtHisD* purification protocol yielded approximately 7.6 mg of homogeneous enzyme having a specific activity value of 1.2 U mg^{-1} with approximately 40-fold purification using three chromatographic steps (Table 1). SDS-PAGE analysis of total protein content for each chromatographic step is shown in Fig. 2.

N-terminal amino acid sequencing, electrospray ionization mass spectrometry (ESI-MS) analysis, and oligomeric state determination

The first 22 N-terminal amino acid residues were identified as MLTRIDLRLGAEELRAALP by Edman degradation sequencing method, in agreement to the *Rv1599* protein-encoded sequence available in the Tuberculist database (<http://www.genolist.pasteur.fr/TubercuList/>). This result unambiguously identifies the purified protein as *MtHisD*, since the first 22 N-terminal amino acids of HisD from *E. coli* are MSFNTIIDWNSCTAEQQQRQLLM.

A value of 45,348.17 Da for the subunit molecular mass of recombinant *MtHisD* was determined by ESI-MS, which is in reasonably good agreement with the theoretical mass value of 45,378.2 Da. The ESI-MS result also revealed no peak at the expected mass of *E. coli* HisD (46,110.3 Da), thus providing support for the identity of purified recombinant protein. The Edman degradation and ESI-MS results are also consistent with no post-translational removal of N-terminal methionine residue (131.2 Da).

A value of 101.8 kDa for the molecular mass of homogeneous recombinant *MtHisD* was estimated by gel filtration chromatography (data not shown). This result demonstrates that *MtHisD* is a dimer in solution, in agreement with HisD enzymes from other organisms [22,23,44].

Table 2Effect of chelating agents and divalent metal ions on *MtHisD* enzyme activity.

Chelating agent/metal	(mM)	Specific activity (U mg^{-1})	Percentage (%)
Control		1.47	100
EDTA	0.1	1.74	118
	1	1.98	135
	10	1.41	96
1,10-Phenanthroline			
	1	0.68	46
	2	0.38	26
	5	0.05	4
Zn ²⁺	40 ^a	0.74	50
Mn ²⁺	40 ^a	1.90	129
Mg ²⁺	40 ^a	1.07	73
Ca ²⁺	40 ^a	0.97	66

^a Enzyme treated with 5 mM 1,10-phenanthroline and diluted 10-fold prior to assay.

Histidinol dehydrogenase as a metalloenzyme

As an attempt to ascertain whether or not *MtHisD* is a metalloenzyme, EDTA was added to the reaction mixture to observe whether or not there would be a reduction in enzyme activity due to divalent metal capture by the chelating agent. We have previously observed that addition of 0.1 mM of EDTA to *M. tuberculosis* dehydroquinate synthase in the absence of substrates was capable of abolishing enzyme activity after 10 min of incubation [45]. However, direct addition of up to 1 mM EDTA showed no decrease in *MtHisD* enzyme activity and, even after incubating the enzyme with 10 mM EDTA for 40 min, no loss of enzyme activity could be observed (Table 2). Similar results have been observed for HisD from *S. typhimurium* [13], from which metal content removal was achieved using 1,10-phenanthroline. Accordingly, 1 mM 1,10-phenanthroline was added to the reaction mixture resulting in a reduction of 46% in *MtHisD* enzyme activity in comparison to control (Table 2). However, measurements of time-dependent inactivation of enzyme activity demonstrated that there is a need to pre-incubate *MtHisD* in the presence of 1 mM 1,10-phenanthroline for approximately 30 min to completely inactivate the enzyme. Pre-incubation of *MtHisD* with 5 mM 1,10-phenanthroline for 3 min resulted in complete loss of enzyme activity. These results suggest that *MtHisD* may contain a tightly bound metal that plays an important role in the catalytic activity, which could not be sequestered by EDTA but could be removed by 1,10-phenanthroline.

To evaluate divalent metal ions that could possibly rescue *MtHisD* activity, recombinant enzyme was pre-incubated with 5 mM 1,10-phenanthroline for 5 min and diluted 10-fold before measuring enzyme activity. Interestingly, even upon dilution and in the absence of any metal, very low enzyme activity was observed for *MtHisD* treated with 1,10-phenanthroline (data not shown). Addition of Ca²⁺, Mg²⁺, Mn²⁺ and Zn²⁺ (40 mM) resulted in regain of *MtHisD* activity (Table 2), whereas no enzyme activity could be rescued upon addition of Cd²⁺, Co²⁺ and Ni²⁺ (40 mM) (data not shown), as has been reported for *S. typhimurium* [13] and cabbage [46] enzymes.

Preliminary analysis to assess metal ion content indicated only the presence of Zn²⁺, in concentrations above 500 ppm. Metal concentration analysis by ICP-AES yielded the following results: Zn²⁺, 6.52 mg L⁻¹ (99.6 μM) and Mn²⁺, <0.001 mg L⁻¹. These results suggest a 0.56 ratio (99.6 μM/176.3 μM) of zinc per subunit. These results are in agreement with previously reported data for *S. typhimurium* [13] and *B. oleracea* [47] enzymes. However, the ICP-AES data are somewhat puzzling as 40 mM Mn²⁺ could rescue *MtHisD* enzyme activity more efficiently than 40 mM Zn²⁺.

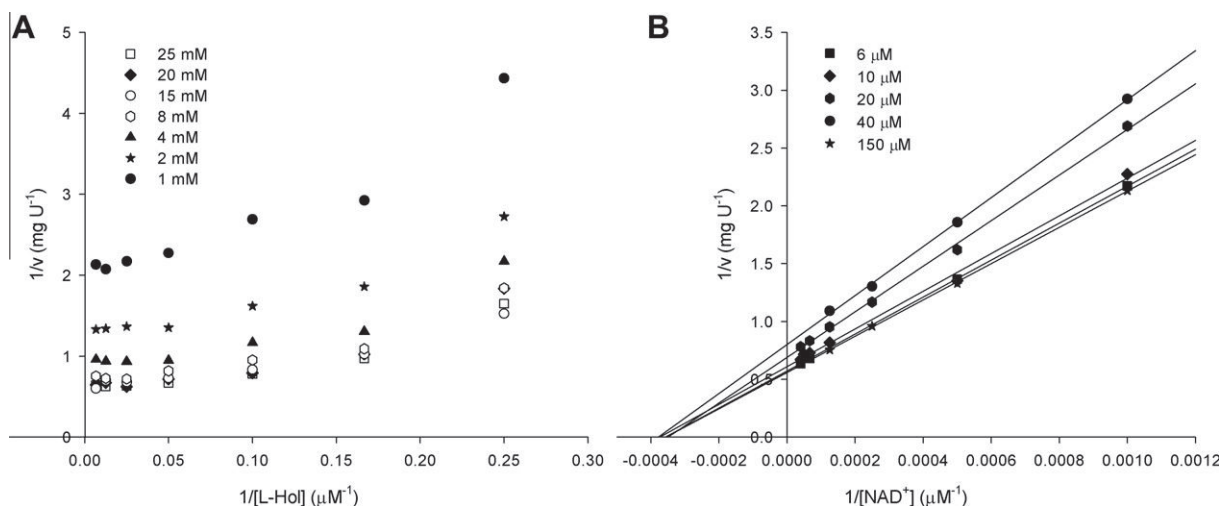


Fig. 3. Double-reciprocal plots of initial velocity experiments. (A) Varying L-Hol concentration at fixed-varied concentrations of NAD $^{+}$. (B) Varying and NAD $^{+}$, concentration at fixed-varied concentrations of L-Hol. Fixed-varied concentrations of substrates are shown in each graph.

(Table 2). It thus appears not to be warranted to affirm that MtHisD is a Zn $^{2+}$ -dependent enzyme. HisD isolated from spring cabbage heads was shown to be Mn $^{2+}$ -dependent [46]. How to reconcile these apparently contradictory results? A possible explanation is that MtHisD (here reported) was produced as a recombinant protein in *E. coli*, and hence being restricted to the metal content of the host or growth media. The *E. coli* system to import manganese is weakly expressed [48], thereby keeping low intracellular levels of this metal, which could explain why we were unable to demonstrate the presence of Mn $^{2+}$ associated to MtHisD enzyme. It has been demonstrated that Mn $^{2+}$ can promptly replace Zn $^{2+}$ in *S. typhimurium* HisD enzyme [13]. However, it has been pointed out that the physiological functions of Mn $^{2+}$ in *M. tuberculosis* are still poorly understood, and that several enzyme systems may prove to be Mn $^{2+}$ -dependent however [49].

Steady state kinetics, ITC and enzyme mechanism

The overall reaction catalyzed by HisD can be analyzed as a ter-reactant system in which NAD $^{+}$ binds twice to the enzyme during the course of the reaction, and participation of water is ignored as its concentration remains constant. Lineweaver-Burk plots showed a parabolic family of lines for varying L-Hol concentrations and fixed-varied NAD $^{+}$ concentrations (Fig. 3A), and a linear pattern of lines was observed for varying NAD $^{+}$ concentrations at fixed-varied L-Hol concentrations (Fig. 3B). The double-reciprocal plots for sequential mechanisms that involve MtHisD:L-Hol:2NAD $^{+}$ quaternary complex formation would display a non-linear dependence on NAD $^{+}$ concentration, including Ordered Ter Ter, partially Random Ter Ter and the completely Random Ter Ter mechanisms [50]. On the other hand, for random mechanisms under steady-state conditions the double-reciprocal plot would show a non-linear dependence on the concentration of L-Hol, even though it binds only once during the reaction sequence [50]. The linear intersecting lines observed for $1/[NAD^{+}]$ and the parabolic family of lines for $1/[L\text{-Hol}]$ may also suggest that MtHisD follows a Ping-Pong mechanism [24]. There are three possible Ping-Pong mechanisms: Bi Uni Uni Bi, Bi Bi Uni Uni, and Hexa Uni [50]. The latter may be discarded as it would give a pattern of parallel lines in double-reciprocal plots for both substrates. A Bi Bi Uni Uni Ping-Pong mechanism would imply that the enzyme would have to exist as a complex with NADH [50]. The value of 45,348.17 Da for the subunit molecular mass of recombinant MtHisD determined by

ESI-MS is consistent with the absence of NADH tightly bound to the enzyme as this value should be approximately 46,043.6 Da (45378.2 + 665.4). Accordingly, the initial velocity data were best fitted to Eq. (2) for a Bi Uni Uni Bi Ping-Pong mechanism, yielding values of $1.45 (\pm 0.04) \text{ s}^{-1}$ for k_{cat} , $4.9 (\pm 0.6) \times 10^{-6} \text{ M}$ for K_M of L-Hol, and $1.4 (\pm 0.1) \times 10^{-3} \text{ M}$ for K_M of NAD $^{+}$.

However, steady-state kinetic data alone could not rule out the random mechanism. Of course, no mechanism is ever proved solely by steady-state kinetic data; at best one can say that given the current data the likely mechanism for MtHisD may be either random or double displacement (Bi Uni Uni Bi Ping-Pong). Equilibrium binary complex formation studies were thus assessed by ITC measurements to both provide thermodynamic signatures of non-covalent interactions to each substrate(s)/product(s) binding processes and distinguish between the possible enzyme mechanisms. No binding of NAD $^{+}$ or NADH to free MtHisD enzyme could be detected by ITC measurements (Fig. 4). On the other hand, ITC measurements showed binding of L-Hol and L-His to free MtHisD enzyme (Fig. 4). These results support a Bi Uni Uni Bi Ping-Pong mechanism in which L-Hol substrate binds to free enzyme followed by NAD $^{+}$ to form a MtHisD:L-Hol:NAD $^{+}$ ternary complex that converts L-Hol into L-His and release of NADH from the MtHisD:L-Hol:NADH ternary complex (Fig. 1B). A second NAD $^{+}$ molecule binds to MtHisD:L-Hol binary complex to form MtHisD:L-Hol:NAD $^{+}$ that converts L-Hol into L-His in the presence of a water molecule followed by release of NADH from MtHisD:L-His:NADH ternary complex yielding the MtHisD:L-His binary complex, from which L-His dissociates to give free MtHisD enzyme for the next round of catalysis (Fig. 1B). It should be pointed out that although the heat flux did not allow reliable estimates for the thermodynamic constants of MtHisD:L-His binary complex formation, it was possible to observe small heat changes between the binding reaction and the control measurement. These data may indicate a large value for the overall dissociation constant for MtHisD:L-His binary complex formation. In any case, the formation of the MtHisD:L-Hol binary complex showed heat changes upon ligand titration (Fig. 4). Fitting the data to one set of sites model yielded the following values for thermodynamic signature of non-covalent interactions upon binary complex formation: net unfavorable enthalpy ($\Delta H = 3.6 \pm 0.5 \text{ kcal/mol}$), favorable entropy ($\Delta S = 35 \pm 13 \text{ cal/mol K}$), and favorable Gibbs energy ($\Delta G = -7 \pm 3 \text{ kcal/mol}$). In addition, the value of $9 (\pm 3) \mu\text{M}$ for the overall dissociation constant at equilibrium of L-Hol binding to MtHisD is in good

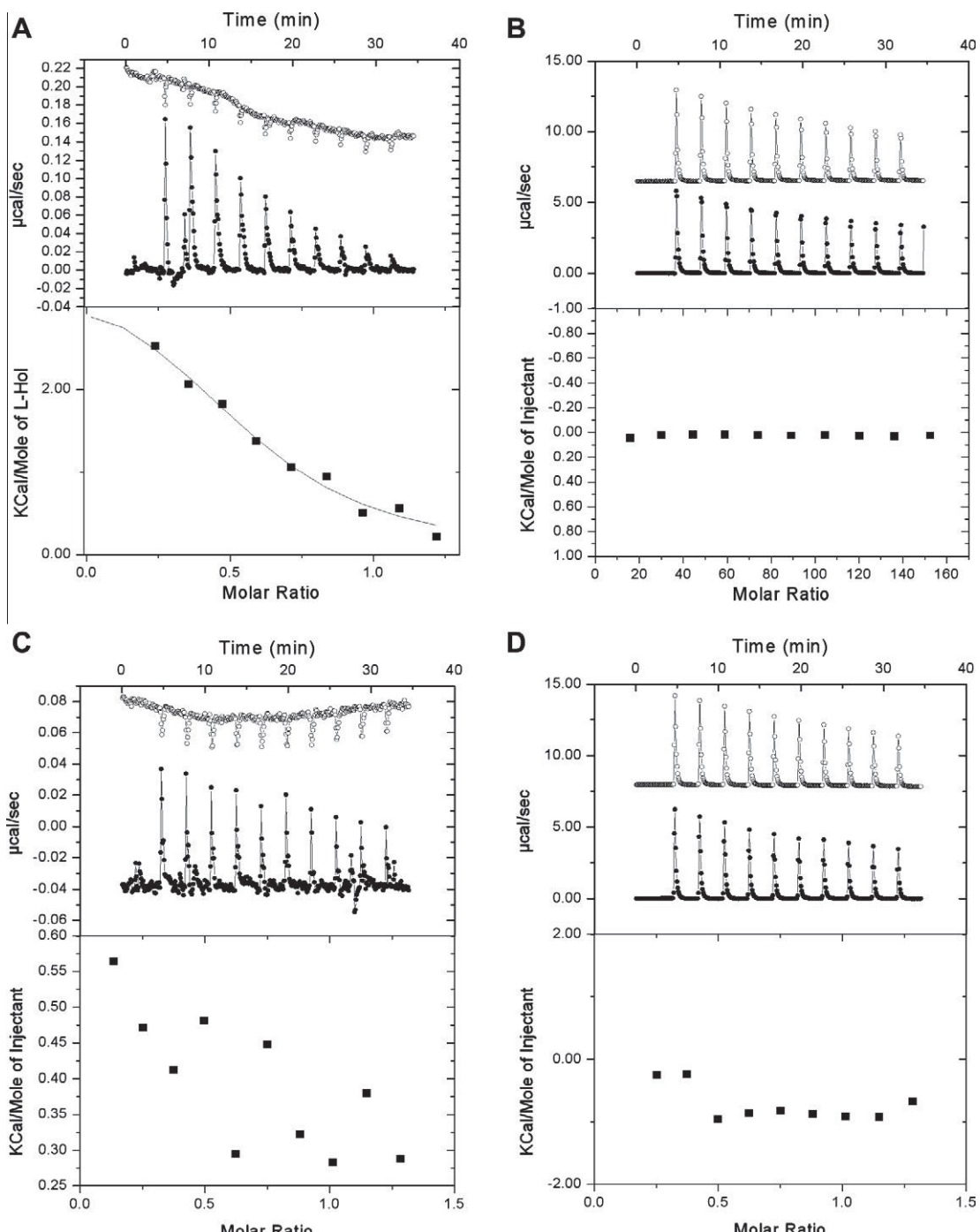


Fig. 4. Isothermal titration calorimetry (ITC) curves for binding of (A) L-Hol (400 μ M), (B) NAD⁺ (50 mM), (C) L-His (800 μ M), and (D) NADH (50 mM) to recombinant MtHisD (69 μ M). Control experiments are shown as empty circles and titration in the presence of enzyme as filled circles.

agreement with the kinetic data ($K_M = 4.9 \mu\text{M}$). Interestingly, the unfavorable enthalpy was off-set by the large favorable entropy, resulting in low equilibrium dissociation constant and a spontaneous reaction (ΔG favorable). The observed positive (unfavorable) enthalpy value for MtHisD:L-Hol formation may be due to an unfavorable redistribution of the network of interatomic interactions (e.g., hydrogen bonds and van der Walls) between the reacting species (including solvent) [51]. The observed positive (favorable) entropy value for L-Hol binding to free MtHisD may be associated with release of “bound” water molecules from the surface to the bulk solvent [51].

pH-rate profiles

To probe for acid-base catalysis, pH dependence studies of k_{cat} , and k_{cat}/K_M for L-Hol and NAD⁺ were performed. The pH-rate data for k_{cat} were fitted to Eq. (4), indicating that protonation of a group (slope of +1) with an apparent pK value of approximately 8 (± 1) (Fig. 5) abolishes catalysis. The pH-rate data for k_{cat}/K_M for L-Hol were fitted to Eq. (4), suggesting that protonation of a group (slope of +1) with an apparent pK value of approximately 8 (± 3) is required for binding of L-Hol to free MtHisD (Fig. 5). These pK_a values may be attributed to conserved histidine residues present

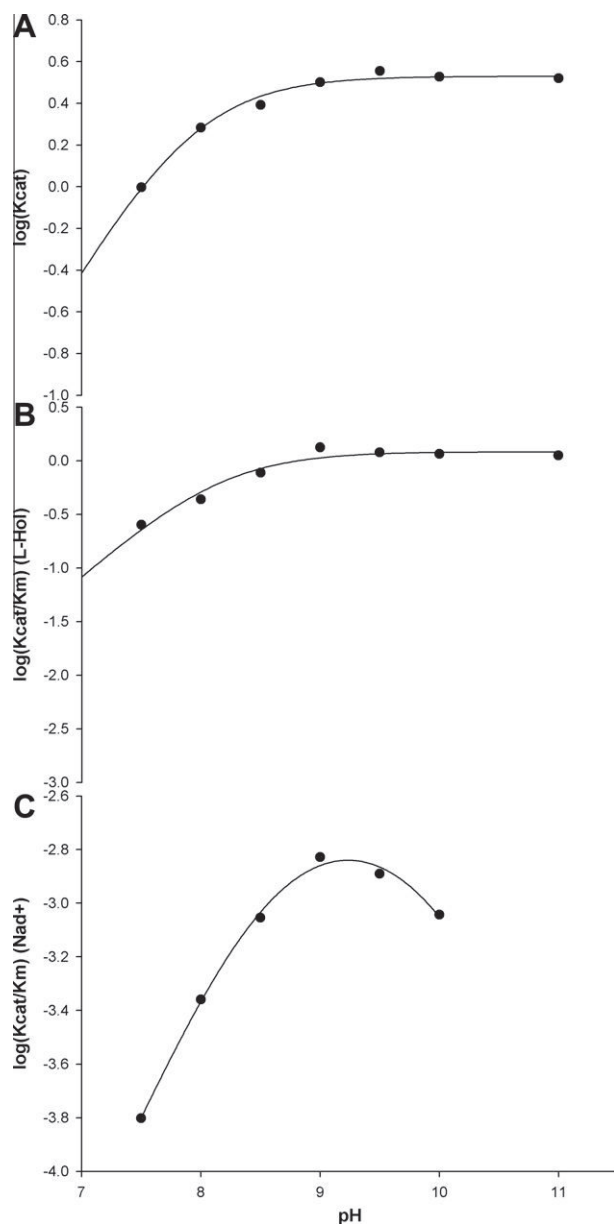


Fig. 5. pH-rate profiles for the reaction catalyzed by *MtHisD*. Steady-state kinetic constants were plotted in the logarithmic form against the pH value of the assay mixture. (A) pH dependence of $\log k_{\text{cat}}$ data were fitted to Eq. (4); (B) pH dependence data of k_{cat}/K_M for l-Hol were fitted to Eq. (4); (C) pH dependence data of k_{cat}/K_M for NAD⁺ were best fitted to Eq. (5).

in the active site (Fig. 6). Although the observed pK values for imidazole side chain of l-His range from 6.0 to 7.0, amino acid residues in biologically active proteins may have very different chemical properties. A number of reports have shown similar pH profiles suggesting that the side chain of histidine residue acts as a base assisting the proton transfers during the overall catalysis [47,52,53]. For instance, a value of $\log(k_{\text{cat}})$ and $\log(k_{\text{cat}}/K_M)$ titration profiles for the overall reaction with l-Hol as the variable substrate indicated that the deprotonated form of a single ionizable group with pK of 8.17 and 8.35 was essential for, respectively, catalysis and substrate binding to *S. typhimurium* HisD [52]. Essential roles for histidines in HisD mode of action have also been shown by site-directed mutagenesis [47,53] and structural studies [23]. The crystal structure of *E. coli* HisD [23] showed that the hydroxyl group of l-Hol forms H-bonds to the backbone carbonyl of

His367 (corresponding to His376 in *MtHisD*) and to the His327^{Nε2} atom (corresponding to His336 in *MtHisD*). It is thus tempting to suggest that the conserved imidazole group of His336 plays a critical role in both catalysis and l-Hol binding to *MtHisD*. The data for k_{cat}/K_M for NAD⁺ were best fitted to Eq. (5), which describes a bell-shaped pH-rate profile for a single ionizing group in the acidic limb that must be unprotonated for NAD⁺ binding and participation of a single ionizing group in the basic limb that must be protonated for substrate binding. These pK values differ by less than a pH unit however. Data fitting yielded an apparent pK value of 9.2, which is a mean of the two residues. The *E. coli* HisD structure showed the phosphate groups of NAD⁺ make H-bonds to Asn211, Tyr130, and Gly133 via a bridging water molecule [23]. The adenosine sugar O2' is H-bonded to Gln188 side chain, whereas O4' interacts with Asn211, and the adenine N3 atom makes an H-bond to Gln188 via a water molecule [23]. The two likely candidates that play a role in NAD⁺ binding to *MtHisD* are the conserved Tyr129 and Tyr223 (Fig. 6). Although the sequence alignment helps infer amino acids involved in catalysis and/or binding, the molecular model (presented in more detail in the next section) suggests that the Tyr129, Tyr223 and His335 residues make contacts with the substrates in the *MtHisD* enzyme active site (Fig. 7). Notwithstanding, the rate expression for k_{cat}/K_M starts with the combination of substrate and enzyme and includes all steps through the first irreversible one, which is usually either release of the first product or an irreversible chemical step prior to this. In addition, the pH-dependent profile for k_{cat} reports on events following the enzyme-substrate complex formation capable of undergoing catalysis, which include the chemical steps, possible enzyme conformational changes, and product release (leading to regeneration of free enzyme). Hence, the ionization of a group observed in the pH profile for k_{cat}/K_M includes both binding and catalytic steps. Accordingly, participation of ionizing groups solely in catalysis cannot be ruled out for the pKs derived from the acidic limbs of the pH profiles for k_{cat}/K_M (Fig. 5B and C). On the other hand, participation of a single ionizing group in the basic limb with apparent pK value of 9.2 derived from the pH profile of k_{cat}/K_M for NAD⁺ can be attributed to substrate binding, as the pH profile for k_{cat} shows no ionizing group involved in catalysis in the basic limb (Fig. 5C). At any rate, site directed mutagenesis efforts should be pursued to assign a definite role in catalysis and/or binding to these amino acid side residues.

Three-dimensional model analysis

The three-dimensional structure of *E. coli* HisD has been determined by X-ray diffraction in the apo state as well as in complex with l-Hol, Zn²⁺ and NAD⁺ at 1.7 Å resolution [23], which was employed as template for molecular homology modeling of *MtHisD* structure. *E. coli* HisD protein sequence is four amino acids shorter than *MtHisD* (434 and 438 amino acids, respectively). Although small gaps were included, there exists high sequence conservation with 36% identity (Fig. 6), which satisfies homology modeling premises [30] and lends support to using *E. coli* HisD as a suitable template. There are no major structural rearrangements upon NAD⁺, l-Hol, and Zn²⁺ binding as compared to the apo form of *E. coli* HisD [23], with RMSD value of just 1 Å when all alpha carbon coordinates are considered. Stereochemical analysis by PROCHECK [33] showed that 91% of *MtHisD* amino acid residues are in the most favored regions of the Ramachandran plot, validating our model as suitable for structural inferences.

Most significant structural variations are observed at the C-termini of each *MtHisD* subunit (RMSD value of 3.08 Å). The HisD monomer consists of four domains; two larger globular domains (domain 1, amino acid residues 25–103, 124–247 and domain 2, amino acids 1–24, 237–381) with an $\alpha/\beta/\alpha$ topology, in which

<i>M. tuberculosis</i>	01	---VLTR---	IDLRGAEALTA AELRAALPRG GADVE-AVLP TVRPIVAAVA ERGAEAALDF GASEDGVRPH AIRVPDAALD AALAGLDCDV CEALQVMVER	93
<i>E. coli</i>	01	--MSFN---	TIIDWNSCTA EQQRQLLMP AISASESITR TVNDILDNVK ARGEDEALREY SAKEDKTCTVT ALKVSAAEIA AASERLSDEL KQAMAVAVKN	94
<i>S. typhimutium</i>	01	--MSFN---	TIIDWNSCTA EQQRQLLMP AISASESITR TVNDILDNVK TRGDDALREY SAKEDKTCTVT ALRVTPEEIA AAGARLSDEL KQAMATAVKN	94
<i>B. oleracea</i>	24	TKKGFVRCMS KSYRLSELSF SQVENLKARP RIDFS-SIFT TVNPPIADAVR SKGDTAVKEY TEREDKVQLN KVVEDVSELID IP--ELDSAV KEAFDVAYDN	120	
		:	.	..
<i>M. tuberculosis</i>	94	TRAVHSGQRR TDVTTTLGPG ATVTERWVPP ERVGLYVPGG NAVVPPSSVM NVVPAQAAVG DSVVVASPPQ AQWDGMHPHT ILAAARLLGV DEVVAVGGQA	193	
<i>E. coli</i>	95	IETFHQAQL PPVDVETQPG VRCQQVTRPV ASVGLYVPGG SAPLFSTVLM LATPASIAGC KKVLCSPPP -----IADE ILYAAQLCGV QDVNVGGQA	198	
<i>S. typhimutium</i>	95	IETFHSAQTL PPVDVETQPG VRCQQVTRPV SSVGLYVPGG SAPLFSTVLM LATPASIAGC KKVLCSPPP -----IADE ILYAAQLCGV QEIFNVGGQA	198	
<i>B. oleracea</i>	121	IYAFHFAQMS TEKSVENMRS VRCKRVRSI GSVGLYVPGG TAVLPSTALM LAIPAQIAGC KTIVLAPPTP KEGS--ICKE VLYCAKRAVG THILKAGGA	218	
		:	.	..
<i>M. tuberculosis</i>	194	AVALLAYGGT DTDGAALTPV DMITGPGNII VTAAKRLCRS R---VGIDAE AGPTEIAIALA DHTADPVHVA ADLISQAEGD ELAASVLVTP -SEDLADATD	269	
<i>E. coli</i>	189	AIAALAFG-- -TE--SVPKV DKIFGPGNMF VTEAKRQVSQ RLDGAAIDMP AGPSEVLVIA DSQATPDFAV SDLISQAEGD PDSQVILLTP -AADMARVA	262	
<i>S. typhimutium</i>	189	AIAALAFG-- -SE--SVPKV DKIFGPGNMF VTEAKRQVSQ RLDGAAIDMP AGPSEVLVIA DSQATPDFAV SDLISQAEGD PDSQVILLTP -DADIARKVA	262	
<i>B. oleracea</i>	219	AIAAMAWG-- -TD--SCPKV EKIFGPGNQY VTAAKMILQN SEAMVSIIDMP AGPSEVLVIA DEHASPVYIA ADLISQAEGD PDSQVVLVVV GDGVNLKATE	313	
		:	*	..
<i>M. tuberculosis</i>	290	AELAGQLOTT VHRERVTAAL TGROSAIVLV DDVDAAVLTVV NAYAAEHELI QTADAPQVAS RIRSAGAIFV GPWSPVSLGD YCAGSNHVLP TAGCARHSSG	389	
<i>E. coli</i>	289	EAVERQLAEL PRAETARQAL N--ASRLIVT KDLAQCVVIS NYQGPHEHII QTRNARELVD SITSAGSVFL GDWSFPESAGD YASGTNHVLP TYGYTATCSS	380	
<i>S. typhimutium</i>	289	EAVERQLAEL PRADTARQAL S--ASRLIVT KDLAQCVVIS NYQGPHEHII QTRNARELVD AITSAGSVFL GDWSFPESAGD YASGTNHVLP TYGYTATCSS	380	
<i>B. oleracea</i>	314	EEIAKQCKSL PRGEFASKL S--HSTVFA RDIMEAITFS NLYAPEHII NVKDAEKWEG LIENAGSVFI GPWSPVSLGD YASGTNHVLP TYGYARMYSG	411	
		:	*	..

Fig. 6. Neighbor-joining multi sequence alignment of *M. tuberculosis* (TubercuList: Rv1599), *E. coli* (UniProt: P06988), *S. typhimurium* (GenBank: NP_461017.1) and *B. oleracea* (GenBank: AAA32991.1) HisD enzymes, performed with ClustalW (1). *B. oleracea* first 23 amino acids were omitted from alignment. Amino acid conservation, strong similarity, weak similarity and in/del are denoted as, respectively, *, :, .., and -. Amino acids involved in substrates binding are shaded in gray.

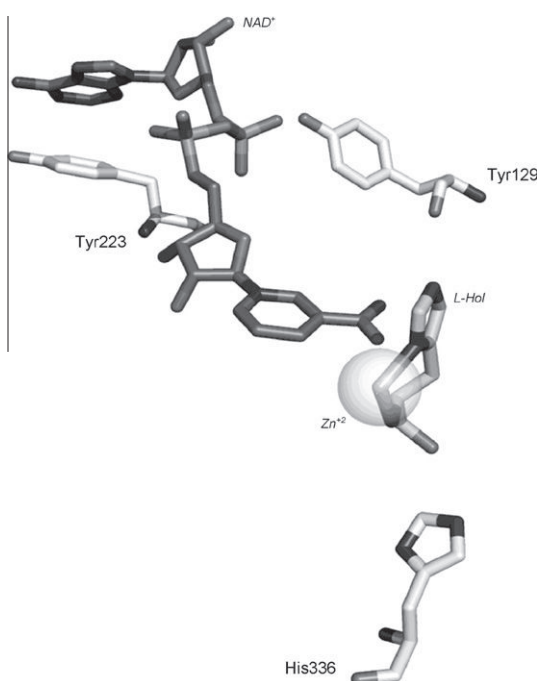


Fig. 7. Proposed MtHisD residues involved in substrate binding and/or catalysis. All residues are less than 4.0 Å from substrates.

the core of both globular domains adopt incomplete Rossmann folds lacking one strand-helix hairpin. A third domain (domain 3, amino acids 104–123 and 400–409) is composed by a three-stranded antiparallel β-sheet that extends away from the two globular domains. The fourth domain (domain 4, residues 410–437) folds into a small V-shaped two-helical hairpin that is perpendicular to the third domain antiparallel β-sheet (Fig. 8A). Structural variation is observed at the C-termini, explicitly at domain 4, where the second helix of the helical hairpin has moved away from

the substrate and Zn²⁺ binding site (Fig. 8B). This displacement of ~7 Å of the side chains of the amino acids involved in l-Hol and Zn²⁺ binding may be a result of domain 4 flexibility. The crystallographic structure of *E. coli* HisD showed no major structural rearrangement upon binding of substrates [23].

Substrate and Zn²⁺ binding sites are located on the homodimer interface, NAD⁺ binding site is located at domain 1, at the incomplete Rossmann fold structural motif. MtHisD amino acids involved in l-Hol binding are His336 and His376 from domain 2 and Glu423 of domain 4 (Fig. 6). The Zn²⁺ ion is octahedrally coordinated to Gln267, His270, Asp369, His428, and two ligands from l-Hol. Amino acid residues contributing to NAD⁺ binding include Tyr129, Gly132, and Asn221 (phosphate binding); Gln193 and Asn221 (adenosine sugar binding); and Phe58, Gln193, and Tyr223 (adenine base binding). The conservation of these amino acid residues is noticeable, being all but Tyr223 conserved among MtHisD homologues (Fig. 6). Although not directly involved in HisD catalysis, Zn²⁺ interacts with the amino group of histidinol that has been suggested to play a role in the correct positioning of l-Hol in the enzyme active site [23].

A proposal for the *E. coli* HisD reaction mechanism has been put forward which involves abstraction of the hydroxyl group proton of l-Hol by His327 (MtHisD His336) and concomitant hydride transfer from the reactive carbon (carbon bound to the hydroxyl group that upon hydride transfer adopts the sp² configuration) to NAD⁺, forming l-Hal and transiently protonated His327 (MtHisD His336) [23]. A neighboring water molecule is activated by Glu326 (MtHisD Glu335) to make a nucleophilic attack on the carbonyl carbon with concomitant protonation of aldehyde oxygen by the transiently protonated His327 (MtHisD His336), leading to the formation of an l-histidindiol (gem-diol) intermediate. Hydride transfer to NAD⁺ from now sp³-gem-diol carbon of -CH(OH)₂ intermediate with concomitant proton abstraction from a substrate hydroxyl group by unprotonated His327 (MtHisD His336) form the sp²-carbon of the carboxylate group of l-His. The protonated His327 (MtHisD His336) is thought to donate a proton to a water molecule. NMR studies indicated that the metal ion interacts with the imidazole portion of the substrate and acts as a Lewis acid

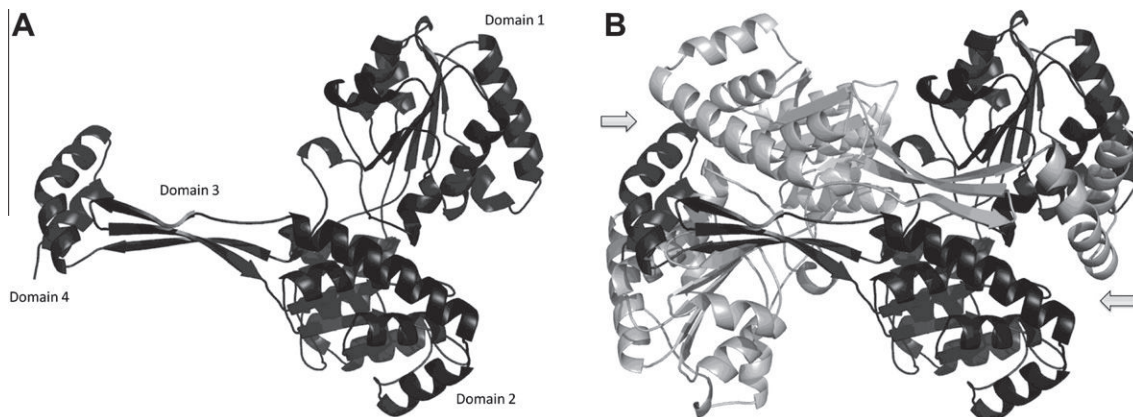


Fig. 8. Molecular model of MtHisD. (A) Three-dimensional structure of the MtHisD monomer, indicating its globular domains (1 and 2), the helical-hairpin (domain 4), and the connective three-stranded antiparallel β -sheet (domain 3). (B) MtHisD homodimeric three-dimensional structure, subunit A in light gray and subunit B in dark gray. The L-shaped arm formed by domains 3 and 4 extends from each monomer and forms a latch-like structure that closes upon domains 1* and 2* of the other monomer (asterisks are residues from the neighboring monomer). The two active sites of MtHisD protein are located at the boundaries of the homodimer interface (arrows). Amino acid residues from both subunits make H- bonds to L-Hol and Zn²⁺ (domains 1, 2, and 4*); and NAD⁺ is H-bonded to amino acids from domain 1.

inducing polarization of the carbonyl group to increase the susceptibility to nucleophilic attack for the aldehyde oxidation [54]. However, structural analysis of *E. coli* HisD prompted the authors to suggest that Zn²⁺ plays a role in proper positioning of L-Hol [23]. As pointed out in the previous section, the conserved imidazole group of His336 is likely the residue with pK value of approximately 8 that plays a critical role in catalysis and L-Hol binding (Fig. 5A and B). A value ranging from 4.3 to 4.5 is usually observed for pK of the γ -carboxyl group of glutamate, although it depends on the chemical context of an enzyme active site. The pH-rate data for MtHisD have not provided a clear evidence for participation of, for instance, Glu335 in either catalysis or substrate binding. Accordingly, site-directed mutagenesis will have to be pursued to reveal whether or not this amino acid side chain plays any role in the mode of action of MtHisD enzyme.

Conclusion

In the present work, PCR amplification, cloning and sequencing of *hisD* gene from *M. tuberculosis* H37Rv strain are described. Data on recombinant MtHisD protein purification, N-terminal amino acid sequencing and electrospray ionization mass spectrometry analyses were presented to confirm the identity of the recombinant protein. Analytical gel filtration, inactivation by chelating agents, activation by divalent metal ions, and inductively coupled plasma atomic emission spectroscopy (ICP-AES) analysis of metal content indicated that MtHisD is a homodimeric metalloprotein. Steady-state kinetics and ITC studies suggested that MtHisD follows a Bi Uni Uni Bi Ping-Pong mechanism, in which L-Hol substrate binds to free enzyme followed by NAD⁺ to form a MtHisD:L-Hol:NAD⁺ ternary complex that converts L-Hol into L-Hal and release of NADH from the MtHisD:L-Hal:NADH ternary complex. A second NAD⁺ molecule binds to MtHisD:L-Hal binary complex to form MtHisD:L-Hal:NAD⁺ that converts L-Hal into L-His in the presence of a water molecule followed by release of NADH from MtHisD:L-His:NADH ternary complex yielding the MtHisD:L-His binary complex, from which L-His dissociates to give free MtHisD enzyme for the next round of catalysis. Based on pH-rate profiles, primary sequence comparisons, and molecular homology modeling of MtHisD, the likely amino acid residues involved in acid-base catalysis and/or substrate binding are proposed. Further efforts to provide a more detailed picture of MtHisD mode of action will include, but not be limited to, site-directed

mutagenesis, chemical rescue, isotope effects, pre-steady state kinetics, and crystal structure determination.

Acknowledgments

This work was supported by funds of Decit/SCTIE/MS-MCT-CNPq-FNDCT-CAPES to National Institute of Science and Technology on Tuberculosis (INCT-TB) to D.S.S. and L.A.B. L.A.B. and D.S.S. also acknowledge financial support awarded by FAPERGS-CNPq-PRONEX-2009. D.S.S. (CNPq, 304051/1975-06) and L.A.B. (CNPq, 520182/99-5) and are Research Career Awardees of the National Research Council of Brazil (CNPq). J.E.S.N. and L.A.R. acknowledge scholarships awarded by CNPq. A.B. acknowledges a scholarship awarded by BNDES.

References

- [1] World Health Organization, Global tuberculosis control: WHO report 2010, Geneva, Switzerland, WHO/HTM/TB/2010.7.
- [2] World Health Organization, Global tuberculosis control: epidemiology, strategy, financing, WHO report 2009, Geneva, Switzerland, WHO/HTM/TB/2009.411.
- [3] D. Kumar, K.V.S. Rao, Regulation between survival persistence, *Microbes Infect.* 13 (2011) 121–133.
- [4] A.A. Velayati, P. Farnia, M.R. Masjedi, T.A. Ibrahim, P. Tabarsi, R.Z. Haroun, H.O. Kuan, J. Ghanavi, P. Farnia, M. Varahram, Totally drug-resistant tuberculosis strains: evidence of adaptation at the cellular level., *Eur. Resp. J.* 34 (2009) 1202–1203.
- [5] A.A. Velayati, *Chest* 136 (2009) 420–425.
- [6] A. Koul, E. Arnoult, N. Lounis, J. Guillermont, K. Andries, *Nature* 469 (2011) 483–490.
- [7] M.E. Winkler, Biosynthesis of Histidine, in: F.C. Neidhardt (Ed.), *Escherichia coli and Salmonella: Cellular and Molecular Biology*, ASM Press, Washington, DC, 1996, pp. 485–505.
- [8] E. Adams, *J. Biol. Chem.* 209 (1954) 829–846.
- [9] E. Adams, *J. Biol. Chem.* 217 (1955) 325–344.
- [10] J.C. Loper, E. Adams, *J. Biol. Chem.* 240 (1965) 788–795.
- [11] S.Y. Lee, C.T. Grubmeyer, *J. Bacteriol.* 169 (1987) 3938–3944.
- [12] A. Nagai, K. Suzuki, E. Ward, M. Moyer, M. Hashimoto, J. Mano, D. Ohta, A. Scheidegger, *Arch. Biochem. Biophys.* 295 (1992) 235–239.
- [13] C. Grubmeyer, M. Skiadopoulos, A.E. Senior, *Arch. Biochem. Biophys.* 272 (1989) 311–317.
- [14] D. Voet, J.D. Voet, Amino acid metabolism, in: D. Voet, J.D. Voet (Eds.), *Biochemistry*, John Wiley & Sons, Inc., USA, 1995, pp. 727–784.
- [15] S.T. Cole, R. Brosch, J. Parkhill, T. Garnier, C. Churcher, D. Harris, S.V. Gordon, K. Eiglmeier, S. Gas, C.E. Barry III, F. Teklaia, K. Badcock, D. Basham, D. Brown, T. Chillingworth, R. Connor, R. Davies, K. Devlin, T. Feltwell, S. Gentles, N. Hamlin, S. Holroyd, T. Hornsby, K. Jagels, B.G. Barrell, *Nature* 393 (1998) 537–544.
- [16] T. Parish, *J. Bacteriol.* 185 (2003) 6702–6706.
- [17] C.M. Sassetti, D.H. Boyd, E.J. Rubin, *Mol. Microbiol.* 48 (2003) 77–84.
- [18] T. Parish, B.G. Gordhan, R.A. McAdam, K. Duncan, V. Mizrahi, N.G. Stoker, *Microbiology* 145 (1999) 3497–3503.

- [19] F. Agüero, B. Al-Lazikani, M. Aslett, M. Berriman, F.S. Buckner, R.K. Campbell, S. Carmona, I.M. Carruthers, A.W.E. Chan, F. Chen, G.J. Crowther, M.A. Doyle, C. Hertz-Fowler, A.L. Hopkins, G. McAllister, S. Nwaka, J.P. Overington, A. Pain, G.V. Paolini, U. Pieper, S.A. Ralph, A. Riechers, D.S. Roos, A. Sali, D. Shanmugam, T. Suzuki, W.C. Van Voorhis, C.L.M.J. Verlinde, *Nat. Rev. Drug Discov.* 7 (2008) 900–907.
- [20] M.M. Bradford, *Anal. Biochem.* 72 (1976) 248–254.
- [21] H. Chassaigne, R. Lobinski, *Analyst* 123 (1998) 2125–2130.
- [22] A. Kheirloomojo, J. Mano, A. Nagai, A. Ogawa, G. Iwasaki, D. Ohta, *Arch. Biochem. Biophys.* 312 (1994) 493–500.
- [23] J.A.R.G. Barbosa, J. Sivaraman, Y. Li, R. Larocque, A. Matte, J.D. Schrag, M. Cygler, *Proc. Natl. Acad. Sci. USA* 99 (2002) 1859–1864.
- [24] I.H. Segel, *Enzyme Kinetics – Behavior Analysis of Rapid Equilibrium and Steady-state Enzyme Systems*, Wiley, Classics Library Edition, Wiley-Interscience Publication, John Wiley & Sons, Inc., New York, 1993.
- [25] P.F. Cook, W.W. Cleland, *Enzyme Kinetics and Mechanism*, Garland Science, New York, 2007.
- [26] S.F. Altschul, T.L. Madden, A.A. Schäffer, J. Zhang, Z. Zhang, W. Miller, D.J. Lipman, *Nucleic Acids Res.* 25 (1997) 3389–3402.
- [27] H.M. Berman, J. Westbrook, Z. Feng, G. Gilliland, T.N. Bhat, H. Weissig, I.N. Shindyalov, P.E. Bourne, *Nucleic Acids Res.* 28 (2000) 235–242.
- [28] J.D. Thompson, D.G. Higgins, T.J. Gibson, *Nucleic Acids Res.* 22 (1994) 4673–4680.
- [29] A. Šali, T.L. Blundell, *J. Mol. Biol.* 234 (1993) 779–815.
- [30] M.A. Martí-Renom, A.C. Stuart, A. Fiser, R. Sánchez, F. Melo, A. Šali, *Annu. Rev. Biophys. Biomol. Struct.* 29 (2000) 291–325.
- [31] A. Šali, J.P. Overington, *Protein Sci.* 3 (1994) 1582–1596.
- [32] M.Y. Shen, A. Šali, *Protein Sci.* 15 (2006) 2507–2524.
- [33] R.A. Laskowski, M.W. MacArthur, D.S. Moss, J.M. Thornton, *J. Appl. Cryst.* 26 (1993) 283–291.
- [34] D.A. Case, D.A. Pearlman, J.W. Caldwell, T.E. Cheatham III, J. Wang, W.S. Ross, C.L. Simmerling, T.A. Darden, K.M. Merz, R.V. Stanton, A.L. Cheng, J.J. Vincent, M. Crowley, V. Tsui, H. Gohlke, R.J. Radmer, Y. Duan, J. Pitera, I. Massova, G.L. Seibel, U.C. Singh, P.K. Weiner, P.A. Kollman, *AMBER 7*. University of California, San Francisco, 2002.
- [35] D. van der Spoel, E. Lindahl, B. Hess, G. Groenhof, A.E. Mark, H.J.C. Berendsen, *J. Comp. Chem.* 26 (2005) 1701–1718.
- [36] W.L. DeLano, *The PyMOL Molecular Graphics System*. DeLano Scientific, San Carlos, CA, USA, 2002, Available from: <<http://www.pymol.org>>.
- [37] P.R. Winship, *Nucleic Acids Res.* 17 (1989) 1266.
- [38] K.C. Kelley, K.J. Huestis, D.A. Austen, C.T. Sanderson, M.A. Donoghue, S.K. Stickel, E.S. Kawasaki, M.S. Osburne, *Gene* 156 (1995) 33–36.
- [39] J.S. Oliveira, C.A. Pinto, L.A. Basso, D.S. Santos, *Protein Expr. Purif.* 22 (2001) 430–435.
- [40] M.L. Magalhaes, C.P. Pereira, L.A. Basso, D.S. Santos, *Protein Expr. Purif.* 26 (2002) 59–64.
- [41] R.G. Silva, L.P. Carvalho, J.S. Oliveira, C.A. Pinto, M.A. Mendes, M.S. Palma, L.A. Basso, D.S. Santos, *Protein Expr. Purif.* 27 (2003) 158–164.
- [42] T.H. Grossman, E.S. Kawasaki, S.R. Punreddy, M.S. Osburne, *Gene* 209 (1998) 95–103.
- [43] F.W. Studier, *Protein Expr. Purif.* 41 (2005) 207–234.
- [44] E. Burger, H. Görisch, F. Lingens, *Biochem. J.* 181 (1979) 771–774.
- [45] J.D. de Mendonça, O. Adachi, L.A. Rosado, R.G. Ducati, D.S. Santos, L.A. Basso, *Mol. BioSyst.* 7 (2011) 119–128.
- [46] A. Nagai, A. Scheidegger, *Arch. Biochem. Biophys.* 284 (1991) 127–132.
- [47] A. Nagai, D. Ohta, *J. Biochem.* 115 (1994) 22–25.
- [48] A. Anjem, S. Varghese, J.A. Imlay, *Mol. Microbiol.* 72 (2009) 844–858.
- [49] D. Agranoff, S. Krishna, *Front. Biosci.* 9 (2004) 2996–3006.
- [50] H. Görisch, *Biochem. J.* 181 (1979) 153–157.
- [51] R. O'Brien, I. Haq, *Applications of Biocalorimetry: Binding, Stability and Enzyme Kinetics*, in: J.E. Ladbury, M.L. Doyle (Eds.), *Biocalorimetry 2: Applications of Calorimetry in the Biological Sciences*, John Wiley & Sons, Ltd., West Sussex, 2004, pp.3–34.
- [52] C. Grubmeyer, H. Teng, *Biochemistry* 38 (1999) 7355–7362.
- [53] H. Teng, C. Grubmeyer, *Biochemistry* 38 (1999) 7363–7371.
- [54] K. Kanaori, N. Uodome, A. Nagai, D. Ohta, A. Ogawa, G. Iwasaki, A.Y. Nosaka, *Biochemistry* 35 (1996) 5949–5954.

Capítulo 04

Considerações Finais

4. CONSIDERAÇÕES FINAIS

As estatísticas divulgadas pela OMS não deixam dúvidas de que a tuberculose é um problema urgente de saúde pública global. Foram 9,4 milhões de casos incidentes de tuberculose em 2009 (WHO report 2010), sendo que no Brasil ocorreram 87 mil destes. Se estes dados já são suficientemente alarmantes, quando consideramos os 440 mil casos de MDR-TB (WHO report 2010), fica clara a necessidade de novas estratégias para combater a tuberculose. Nessa busca, se encontra o desenvolvimento de novas drogas baseadas em alvos moleculares definidos que preferencialmente sejam efetivas também contra as cepas resistentes. A via de biossíntese de histidina surge nesse âmbito oferecendo alvos atrativos, visto que a essencialidade do gene *hisD* do bacilo foi demonstrada por Parish e colaboradores (PARISH *et al.*, 1999). O presente trabalho foi capaz de caracterizar bioquimicamente o produto do gene em questão.

A enzima histidinol desidrogenase foi purificada até a homogeneidade utilizando-se três etapas cromatográficas. A determinação de seu peso molecular e da sua sequência N-terminal corroboram a sua identidade. O peso molecular em solução indica que a enzima se apresenta na forma dimérica, como já foi reportado para outros organismos (BARBOSA *et al.*, 2002; BURGER *et al.*, 1979; KHEIROLOMOOM *et al.*, 1994).

Os estudos de cinética em estado-estacionário indicaram que a enzima necessita de um metal divalente para catalisar a reação, e dentre os metais testados neste trabalho, o Mn²⁺ foi o que demonstrou estimular mais a enzima. A enzima homogênea foi enviada para análise do conteúdo de metal, indicando a presença de Zn²⁺ na amostra. Quando ensaiada na presença de 1,10-Fenantrolina 5 mM, foi observado uma grande diminuição na atividade da enzima, devido ao sequestro do Zn²⁺ presente no sítio ativo.

O padrão de linhas observado no experimento de velocidade inicial, juntamente com os experimentos de ligação utilizando calorimetria de titulação isotérmica (ITC), tornou possível a elucidação do mecanismo catalítico da enzima. A MtHisD segue um mecanismo ordenado conhecido como Ping-pong Bi Uni Uni Bi. A reação começa com a ligação do L-Histidinol, seguido pela primeira

molécula de NAD⁺. O L-Histidinol é convertido a L-Histidinal e então ocorre a liberação da primeira molécula de NADH. A reação prossegue com a entrada da segunda molécula de NAD⁺ no sítio ativo e a conversão do L-Histidinal para L-Histidina. A segunda molécula de NADH é liberada e por último a L-Histidina se desliga da enzima. A constante catalítica (k_{cat}) foi calculada segundo o modelo proposto e o valor encontrado foi de $1,45 \pm 0,04$ s⁻¹. As constantes de Michaelis-Menten encontradas foram de $4,9 \pm 0,6$ μM para o L-Histidinol e $1,4 \pm 0,1$ mM para o NAD⁺. Com os resultados encontrados para o mecanismo da MtHDH, fica claro, devido a ordem de adição dos substratos e a incapacidade do NAD⁺ de se ligar a enzima livre, que qualquer composto desenhado no intuito de inibir a sua atividade deve ser baseado na estrutura do L-Histidinol.

O modelo tridimensional construído auxiliou na análise dos resultados de perfis de pH e permitiu a observação das interações dos substratos com os resíduos presentes no sítio ativo. No entanto, tentativas de cristalização continuam sendo de grande importância, pois permitirão, no futuro, o estudo da interação de compostos que venham a ser inibidores da enzima.

Os resultados agrupados aqui formam uma base sólida para o início do estudo de moléculas inibidoras da atividade da MtHisD. Estudos futuros de efeitos isotópicos, cinética em estado pré-estacionário e mutagênese sítio-dirigida, são necessários para uma maior compreensão da reação catalisada pela enzima MtHisD. O maior conhecimento de toda a catálise auxiliará no desenvolvimento de moléculas mais potentes que possam ser utilizadas no tratamento da tuberculose.

Bibliografia

Aguero, F., Al-Lazikani, B., Aslett, M., Berriman, M., Buckner, F. S., Campbell, R. K., Carmona, S., Carruthers, I. M., Chan, A. W. E., Chen, F., Crowther, G. J., Doyle, M. A., Hertz-Fowler, C., Hopkins, A. L., McAllister, G., Nwaka, S., Overington, J. P., Pain, A., Paolini, G. V., Pieper, U., Ralph, S. A., Riechers, A., Roos, D. S., Sali, A., Shanmugam, D., Suzuki, T., Van Voorhis, W. C., Verlinde, C. L. M. J., (2008) Genomic-scale prioritization of drug targets: the TDR Targets database, *Nat. Rev. Drug Disc.*, 7:900-907.

Alifano, P., Fani, R., Lio, P., Lazcano, A., Bazzicalupo, M., Bruni, C. B., (1996) Histidine Biosynthetic Pathway and Genes: Structure, Regulation, and Evolution. *Microbiol. Rev.* 60: 44-69.

Barbosa, J.A., Sivaraman, J., Li, Y., Larocque, R., Matte, A., Schrag, J.D., Cygler, M. (2002) Mechanism of action and NAD⁺-binding mode revealed by the crystal structure of L-histidinol dehydrogenase. *Proc. Natl. Acad. Sci. USA* 99: 1859-1864.

Bloom, B.R. and Murray, C.J.L. (1992) Tuberculosis: commentary on a reemergent killer. *Science* 257: 1055-1064.

Bradford, M.M., Mcrorie, R.A. and Williams, W.L. (1976) A rapid and sensitive method for the quantitation of microgram quantities of protein utilizing the principle of protein-dye binding. *Anal. Biochem.* 72: 248-254.

Brennan, P.J. and Nikaido, H. (1995) The envelope of Mycobacteria. *Annu. Rev. Biochem.* 64: 29-63.

Brennan, P.J. (1997) Tuberculosis in the context of emerging and reemerging diseases. *FEMS Immunol. Med. Microbiol.* 18: 263-269.

Burger, E., Gorisch, H., Lingens, F., (1979) The Catalytically Active Form of Histidinol Dehydrogenase from *Salmonella typhimurium*, *Biochem. J.* 181: 771-774.

Caws, M. and Drobniowski, F.A. (2001) Molecular techniques in the diagnosis of *Mycobacterium tuberculosis* and the detection of drug resistance. *Ann. N Y Acad. Sci.* 953: 138-145.

Cole, S.T., Brosch, R., Parkhill, J., Garnier, T., Churcher, C., Harris, D., Gordon, S.V., Eiglmeier, K., Gas, S., Barry, C.E. 3rd, Tekaia, F., Badcock, K., Basham, D., Brown, D., Chillingworth, T., Connor, R., Davies, R., Devlin, K., Feltwell, T., Gentles, S., Hamlin, N., Holroyd, S., Hornsby, T., Jagels, K., and Barrell, B.G. (1998) Deciphering the biology of *Mycobacterium tuberculosis* from the complete genome sequence. *Nature* 393: 537-544.

Dorman, S.E. & Chaisson, R.E. From magic bullets back to the Magic Mountain: the rise of extensively drug-resistant tuberculosis, *Nat. Med.* 13 (2007) 295-298.

Ducati RG, Ruffino-Neto A, Basso LA, Santos DS. The resumption of consumption – A review on tuberculosis. *Ment Inst Oswaldo Cruz*. 2006;101:697- 714.

Enarson, D.A. and Murray, J.F. (1996) Global epidemiology of tuberculosis. In: *Tuberculosis* (Rom, W.M. and Garay, S., Eds.), pp. 57-75. Little, Brown and Co., Boston, MA.

Fatkenheuer, G., Taelman, H., Lepage, P., Schwenk, A., and Wenzel, R. (1999) The return of tuberculosis. *Diag. Microbiol. Infect. Dis.* 34: 139-146.

Kheirolomoom, A., Mano, J., Nagai, A., Ogawa, A., Iwasaki, G., and Ohta, D. (1994) Steady-state kinetics of cabbage histidinol dehydrogenase. *Arch. Biochem. Biophys.* 312(2): 493-500.

O'Brien, R.J. & Nunn, P.P. The need for new drugs against tuberculosis, *Am. J. Respir. Crit. Care Med* 162 (2001) 1055-1058.

Palomino JC, Leão SC, Ritacco V. *Tuberculosis* 2007 - From basic science to patient care. Disponível em: <www.TuberculosisTextbook.com>. Acesso em: maio de 2010.

Parish, T. (2003) Starvation survival response of *Mycobacterium tuberculosis*. *J. Bacteriol.* 185: 6702-6706.

Parish, T., Gordhan, B.G., McAdam, R.A., Duncan, K., Mizrahi, V., Stoker, N.G. (1999) Production of mutants in amino acid biosynthesis genes of *Mycobacterium tuberculosis* by homologous recombination. *Microbiol.* 145: 3497-3503.

Pasqualoto, K.F & Ferreira, E.I. An approach for the rational design of new antituberculosis agents, *Curr. Drug Targets* 2 (2001) 427-437.

Petrini, B. and Hoffner, S. (1999) Drug-resistant and multidrug-resistant tubercle bacilli. *Int. J. Antimicrob. Agents* 13: 93-97.

Pieters, J. *Mycobacterium tuberculosis* and the Macrophage: Maintaining a Balance. *Cell Host Microbe*; v. 3, n. 6, p. 399-407, 2008.

Ruffino-Neto, A. (2002) Tuberculosis: the neglected calamity. *Rev. Soc. Brasil. Med. Trop.* 35: 51-58.

Sassetti, C.M., Boyd, D.H., Rubin, E.J. (2003) Genes required for mycobacterial growth defined by high density mutagenesis. *Mol. Microbiol.* 48: 77-84.

Telenti, A. and Iseman, M. (2000) Drug-resistant tuberculosis: what do we do now? *Drugs* 59: 171-179.

World Health Organization, Global tuberculosis control: WHO report 2010, Geneva, Switzerland, WHO/HTM/TB/2010.7.

Winkler, M.E. (1996) Biosynthesis of Histidine. In: *Escherichia coli and Salmonella: Cellular and Molecular Biology* (Neidhardt, F.C., Ed.) ASM Press, Washington, DC, pp. 485-505.

Yew, W.W.; Leung, C.C. Update in tuberculosis 2007. Am. J. Respir. Crit. Care Med.; v.177, n. 5, p. 479-485, 2008. Review.

Zhang, Y and Young, D. (1993) Molecular mechanisms of isoniazid: a drug at the front line of tuberculosis control. Trends Microbiol. 1: 109-113

